JASA ARTICLE

Dynamically orthogonal narrow-angle parabolic equations for stochastic underwater sound propagation. Part I: Theory and schemes

Wael H. Ali[1,2] and Pierre F. J. Lermusiaux[1,2,a)]
[1]Department of Mechanical Engineering, Massachusetts Institute of Technology, Cambridge, Massachusetts 02139, USA
[2]Center for Computational Science and Engineering, Massachusetts Institute of Technology, Cambridge, Massachusetts 02139, USA

ABSTRACT:
Robust informative acoustic predictions require precise knowledge of ocean physics, bathymetry, seabed, and acoustic parameters. However, in realistic applications, this information is uncertain due to sparse and heterogeneous measurements and complex ocean physics. Efficient techniques are thus needed to quantify these uncertainties and predict the stochastic acoustic wave fields. In this work, we derive and implement new stochastic differential equations that predict the acoustic pressure fields and their probability distributions. We start from the stochastic acoustic parabolic equation (PE) and employ the instantaneously-optimal Dynamically Orthogonal (DO) equations theory. We derive stochastic DO-PEs that dynamically reduce and march the dominant multi-dimensional uncertainties respecting the nonlinear governing equations and non-Gaussian statistics. We develop the dynamical reduced-order DO-PEs theory for the Narrow-Angle parabolic equation and implement numerical schemes for discretizing and integrating the stochastic acoustic fields.
https://doi.org/10.1121/10.0024466

(Received 20 November 2023; accepted 21 December 2023; published online 25 January 2024)

[Editor: John A. Colosi] Pages: 640–655

I. INTRODUCTION

Reliable acoustic exploration and navigation in the ocean require precise knowledge of the environmental state (e.g., ocean physics, bathymetry, seabed) and acoustic parameters (e.g., source location and frequencies). When all such information is available, sound waves can be reliably used to explore the ocean and seabed (Baggeroer *et al.*, 1993; Becker *et al.*, 2009; Firing and Gordon, 1990; Gartner, 2004; Medwin and Clay, 1998), to locate underwater objects and animals (Blondel, 2010; Bonnel *et al.*, 2014; Jagannathan *et al.*, 2009; Lavery *et al.*, 2007; MacLennan and Simmonds, 2013; Makris *et al.*, 2006; Quazi, 1981), and to communicate via the oceanic waveguide (Akyildiz *et al.*, 2005; Benjamin *et al.*, 2010; Stojanovic, 1996). However, in many real-world applications, such information is typically incomplete and uncertain (Lermusiaux *et al.*, 2006; Tollefsen, 2021) due to the sparse and heterogeneous data collected (Etter, 2018), as well as to the complex ocean physics and acoustics dynamics, multiscale interactions, and large dimensions (Brekhovskikh and Lysanov, 1982; Duda *et al.*, 2019). This incomplete knowledge leads to several sources of uncertainty in acoustic modeling. The ocean currents, temperature, salinity, and pressure fields, and as a result the sound speed and density fields, are often outputs of ocean physics models with uncertain initial and boundary conditions, and numerical approximations (Lermusiaux *et al.*, 2006; Rixen *et al.*, 2012). The exact bottom topography and properties are not available which adds uncertainties to the acoustic predictions (Dosso *et al.*, 2014; Etter, 2018; Jakobsson *et al.*, 2017; Tolstoy, 1996). Finally, numerical acoustic models are themselves approximations of the original sound wave equations. To represent these uncertainties and incomplete knowledge, stochastic environmental fields force the acoustic models and sound propagation thus becomes stochastic. In this work, we develop principled probabilistic theory and schemes to quantify the effects of uncertainties in ocean physics, bathymetry, and source location in ocean acoustic partial differential equations (PDEs) and predict the propagating stochastic acoustic wave fields and their probability distributions. This is done by deriving and implementing new stochastic dynamically-adaptive differential equations for probabilistic underwater acoustic modeling, starting from the stochastic version of the acoustic Parabolic Equation (PE) (Jensen *et al.*, 2011; Tappert, 1977). The PE is a widely used solution technique for low to mid-frequency acoustic propagation in several models, e.g., FOR3D (Botseas *et al.*, 1987), UMPE (Smith and Tappert, 1993), RAM (Collins, 1995), Peregrine (Heaney and Campbell, 2016), and the three-dimensional (3-D) wide-angle split-step Fourier PE (Lin *et al.*, 2013). Prior progress in stochastic and random media underwater sound propagation is reviewed next and includes the following methods: (i) Monte Carlo (MC) sampling, (ii) Error Subspace Statistical Estimation (ESSE), (iii) Wave Propagation in Random Media (WPRM) theory, (iv) uncertainty transfer

a)Email: pierrel@mit.edu

techniques, (v) Polynomial Chaos (PC) expansions, (vi) Machine Learning (ML) techniques, and (vii) data-driven Dynamic Mode Decompositions (DMDs).

Monte Carlo sampling techniques are the most straightforward and have been widely used in the community (Gerstoft and Mecklenbräuker, 1998; Shorey *et al.*, 1994). Using this method, repeated sampling of the Probability Density Function (PDF) of uncertain model parameters and/or fields is used to construct an ensemble of acoustic field predictions by running multiple deterministic model runs (Liu, 2008). However, a large number of realizations are typically required to capture the multi-dimensional environmental uncertainties making brute force MC computationally infeasible. To address this MC inefficiency, Error Subspace Statistical Estimation (ESSE) focuses on evolving the principal components of the ocean physics and acoustics uncertainties, using an ensemble of appropriately perturbed simulations (Lermusiaux, 2006; Lermusiaux *et al.*, 2002; Lermusiaux *et al.*, 2020a; Lermusiaux *et al.*, 2020b, 2010; Robinson and Lermusiaux, 2004).

An alternative approach for incorporating uncertainties builds on advances in WPRM (Colosi, 2016; Ishimaru, 1978; Uscinski, 1977). Progress in this field includes perturbation methods (Born *et al.*, 1999; Chernov, 2017; Rytov *et al.*, 1987), moment equation methods (Ratilal and Makris, 2005; Tatarskii, 1971; Uscinski, 1977), path integral methods (Colosi *et al.*, 1994; Dashen, 1979; Feynman and Hibbs, 1965; Flatté, 1983), and mode transport theory (Colosi, 2008; Colosi *et al.*, 2013; Creamer, 1996; Dozier and Tappert, 1978a,b; Rouseff *et al.*, 2002). Results have been successfully applied in several idealized and realistic ocean acoustic problems (Colosi, 2016) and transport theory has been very fast when the assumptions are satisfied. However, predicting the full PDF of the stochastic acoustic fields remains challenging as most of these methods rely on equations for only the statistical moments of the quantities of interest. Recently, a PDF propagation technique (James and Dowling, 2005) has been proposed extending PDF transport theories used in the study of turbulence (Pope, 2000). The authors obtain and solve differential equations for the PDF of the acoustic fields from fine-grain PDF equations (James and Dowling, 2005). Although this technique can be computationally efficient compared to MC methods, it has some limitations. First, stochastic equations for realistic ocean and acoustic field PDFs are very high-dimensional and nonlinear, and require closure models (James and Dowling, 2005; Miller, 2007; Pope, 2000). Second, prior knowledge about the PDFs of the input parameter uncertainty is typically not available.

A fourth family of techniques is used to estimate an uncertainty band and/or the PDF of the transmission loss (TL) due to environmental uncertainties. It includes the Uncertainty Band (UBAND) algorithm (Fabre and Wood, 2013; Zingarelli, 2008), the field shifting (FS) method (James and Dowling, 2008), and the *ad hoc* Area Statistics (AS) method (Patterson and Dowling, 2017). The UBAND algorithm estimates an uncertainty bound of TL using the frequency- and range-averaging correspondence introduced by Harrison (Harrison and Harrison, 1995). On the other hand, the FS technique estimates the PDF of TL using the property that on a local scale, small changes in an environmental parameter lead to small spatial shifts in the acoustic field (Dosso *et al.*, 2007). Similar to the UBAND and FS methods, AS uses a reference TL prediction and gathers the TL values within a range-depth box around the receiver location to estimate the PDF of TL at that location. In spite of the computational advantages and adaptability provided by these methods for real-time acoustic uncertainty analysis, their accuracy drops significantly when the underwater environment is complex with large uncertainties, and they cannot be used to compute uncertainty estimates of the phase (James and Dowling, 2008).

PC methods have also been used to predict acoustic field uncertainties (Creamer, 2006; Finette, 2005, 2006; Gerdes and Finette, 2012; James and Dowling, 2011; Khazaie *et al.*, 2019; Khine *et al.*, 2010). They are used for uncertainty quantification (UQ) in fluid (Le Maître *et al.*, 2001; Le Maître and Knio, 2010; Najm, 2009; Xiu and Karniadakis, 2003) and solid mechanics (Doostan *et al.*, 2007; Ghanem and Spanos, 2003; Xiu *et al.*, 2002). With PC, the stochastic acoustic field is written as a PC expansion where the uncertainty is represented by a fixed polynomial basis. The expansion coefficients are obtained by solving a system of coupled PDEs based on the original governing equation. However, challenges arise due to the use of a fixed polynomial basis for capturing the uncertainty, which leads to requiring more terms in the PC expansion, and hence higher computational costs (Khine *et al.*, 2010) and fundamental limitations (Branicki and Majda, 2013).

Most recently, ML techniques have gained significant popularity in underwater acoustic applications (Bianco *et al.*, 2019; Michalopoulou *et al.*, 2021) and have been used for estimating the PDF of TL in representative ocean environments (Lee *et al.*, 2022). This was accomplished by training a neural network on a large dataset of TL predictions at sample receiver locations in ocean environments with various source properties. The NN was then used to estimate the PDF of TL in new ocean environments and provided good accuracy when compared to the PDF obtained using a brute force MC approach. However, the accuracy of the estimates was shown to be lower at short ranges and in the case of multimodal TL distributions. In addition, the expensive efforts undertaken when constructing the large training dataset for all possible ocean environments and acoustic parameters limit the ML model generalization. Last, high-dimensional systems such as those encountered in ocean acoustics have the inherent challenges of multiscale transient dynamics, and many NN architectures cannot readily incorporate physical constraints (e.g., acoustic reciprocity) and encode the global conservation laws. Careful attention must therefore be exercised when applying ML techniques for estimating acoustic uncertainties.

Data-driven DMDs based on Proper Orthogonal Decomposition and Koopman analysis (Schmid, 2022) have

https://doi.org/10.1121/10.0024466

been used to reduce sequences of data, extract dominant features, and build reduced-order dynamical models directly from data. As acoustics structures cover a large range of scales and classic DMD bases do not evolve, their use in acoustics has been limited (El Moçayd *et al.*, 2020; Jourdain *et al.*, 2013). Recent progress in adaptive DMD can however be used to build local stochastic models for forecasting onboard underwater vehicles (Heuss *et al.*, 2020; Ryu *et al.*, 2022; Ryu *et al.*, 2021). Instead of starting from data, our present contribution starts from fundamental acoustics equations.

In Part I of this two-part paper, we derive and implement a new range-dynamic uncertainty quantification methodology for optimal reduced-order stochastic underwater sound propagation, extending the Dynamically Orthogonal (DO) decomposition (Sapsis and Lermusiaux, 2009, 2012; Ueckermann *et al.*, 2013) to acoustics. The DO differential equations have been shown to be an instantaneously-optimal reduction of stochastic dynamical systems (Feppon and Lermusiaux, 2018b, 2019) and this optimality is here broadened to range-dynamic acoustic PEs, for an instantaneously-in-range optimal reduction. Starting from the stochastic PE, we derive the governing DO differential equations that dynamically evolve and reduce acoustic uncertainties in range, respecting the nonlinear stochastic governing PEs and non-Gaussian statistics in the environment and acoustics parameters. The DO-PEs are then developed and implemented for the Narrow-Angle PE (NAPE) (Tappert, 1977) to obtain the DO-NAPE finite-volume framework. In Part II of this two-part paper (Ali and Lermusiaux, 2024), the DO-NAPE framework is applied to three new stochastic canonical tests and validated against analytical solutions and standard MC techniques.

In what follows, the problem statement is provided in Sec. II. In Sec. III, the new optimally-reduced DO-PE acoustics differential equations are obtained and discussed. Their stochastic initial and boundary conditions, their specific properties, their application to the NAPE, the numerical schemes used for their integration, and their computational costs are presented. Section IV discusses key differences between the governing DO-PEs and the coupled and adiabatic normal modes equations. Concluding remarks and discussions are provided in Sec. V.

II. PROBLEM STATEMENT

An uncertain multilayered medium consisting of a stochastic ocean waveguide overlaying one or several fluid sedimental layers in a 3-D space is considered. In addition to the uncertain sound speed, density, and bathymetry fields, the location and frequency of the acoustic source are also uncertain. Due to all these uncertainties, the resulting acoustic pressure field in the domain is also stochastic. For the stochastic space, uncertainties are described with random variables and stochastic fields indexed by the stochastic parameter ξ, which represents an event in the stochastic event space Ξ. For the physical space, following the notation in Lin *et al.* (2013) to unify cylindrical and Cartesian coordinate systems, the position $\boldsymbol{x}$ is written as $\boldsymbol{x} = (\boldsymbol{x}_\perp, \eta)$, where $\boldsymbol{x}_\perp = (x_1, x_2) \in \mathcal{D}$ denotes the two-dimensional transverse coordinates and $\eta \in (0, R]$ the position in the range direction, typically chosen as the dimension in the domain with the weakest variations and/or determined by the location of the instruments with R the total propagation range (Jensen *et al.*, 2011). The stochastic isotropic time-harmonic point sound source of uncertain frequency $f(\xi)$ is located at $\eta = \eta_s(\xi)$ and $\boldsymbol{x}_\perp = \boldsymbol{x}_{\perp,s}(\xi) = (x_{1,s}(\xi), x_{2,s}(\xi))$. Figure 1 illustrates this generic stochastic underwater sound propagation and all sources of uncertainties.

The stochastic acoustic pressure field generated by the harmonic point source at $\eta = \eta_s(\xi)$ is denoted by $p'(\boldsymbol{x}_\perp, \eta; \xi)$. For $\eta > \eta_s(\xi)$, $p'(\boldsymbol{x}_\perp, \eta; \xi)$ satisfies the stochastic elliptic variable-density Helmholtz equation (Bergmann, 1946),

$$\rho \nabla \cdot \left(\frac{1}{\rho} \nabla p' \right) + k_0^2 n_a^2 p' = 0, \tag{1}$$

subject to the appropriate stochastic boundary conditions in the domain of interest. In Eq. (1), $\rho = \rho(\boldsymbol{x}_\perp, \eta; \xi)$ is the stochastic space-varying medium density, $k_0(\xi) = \omega(\xi)/c_0 = 2\pi f(\xi)/c_0$ is a reference wavenumber, n_a is the stochastic complex-valued (accounting for medium attenuation) index of refraction defined as $n_a^2(\boldsymbol{x}_\perp, \eta; \xi) = (c_0/c)^2(1 + ia/27.29)$, $c = c(\boldsymbol{x}_\perp, \eta; \xi)$ is the stochastic space-varying medium sound speed, and $a = a(\boldsymbol{x}_\perp, \eta; \xi)$ is the stochastic attenuation coefficient (in dB/λ).

Defining the density-reduced pressure $p = \rho^{-1/2} p'$, Eq. (1) can be rewritten as the density-reduced Helmholtz equation (Bergmann, 1946),

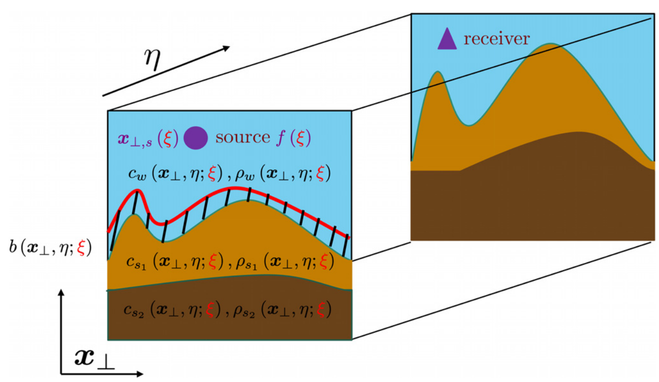

FIG. 1. (Color online) Schematic of the 3D stochastic underwater sound propagation within an uncertain multilayered medium with environmental and acoustic uncertainties. It contains a stochastic ocean waveguide of properties c_w and ρ_w varying in range η and transverse directions $\boldsymbol{x}_\perp$, overlaying one or several seabed layers with properties c_{s_1} and ρ_{s_1}, c_{s_2} and ρ_{s_2}, etc. The stochastic water-seabed interface is defined by the bathymetry field b. An isotropic harmonic point source of frequency f located at range $\eta = 0$ and $\boldsymbol{x}_\perp = \boldsymbol{x}_{\perp,s}$ is emitting sound waves. The acoustic pressure field $\tilde{p}$ at receivers located at any $\boldsymbol{x} = (\boldsymbol{x}_\perp, \eta)$ is sought. As described in the text and stated in the schematic, all these parameters and fields are uncertain and represented by random variables and stochastic fields indexed by the stochastic parameter ξ.

$$\nabla^2 p + k_0^2 n_{eff}^2 p = 0, \tag{2}$$

with the stochastic squared effective index of refraction

$$n_{eff}^2 = n_a^2 + \frac{1}{2k_0^2}\left(\frac{1}{\rho}\nabla^2\rho - \frac{3}{2\rho^2}|\nabla\rho|^2\right). \tag{3}$$

From the solution of Eq. (2), one obtains the stochastic transmission loss,

$$TL(\boldsymbol{x}_\perp, \eta; \xi) = -20\log_{10}\left|\frac{p(\boldsymbol{x}_\perp, \eta; \xi)}{p_0(\xi)}\right|, \tag{4}$$

where $p_0 = \exp(ik_0)/4\pi$ is a nominal pressure value at 1-m distance from the source (Jensen *et al.*, 2011).

Under the PE approximation (Jensen *et al.*, 2011; Tappert, 1977), the acoustic pressure $p(\boldsymbol{x}_\perp, \eta; \xi)$ is decomposed as $p(\boldsymbol{x}_\perp, \eta; \xi) = v(\eta; \xi)\psi(\boldsymbol{x}_\perp, \eta; \xi)$, where $v(\eta; \xi)$ is a function strongly dependent on the range direction η that can be approximated in the far-field as (Jensen *et al.*, 2011; Lin *et al.*, 2013)

$$v(\eta; \xi) \sim \begin{cases} \exp(ik_0(\xi)\eta) & \text{in Cartesian coordinates,} \\ \exp(ik_0(\xi)\eta)/\sqrt{\eta} & \text{in cylindrical coordinates.} \end{cases} \tag{5}$$

In addition, $\psi(\boldsymbol{x}_\perp, \eta; \xi)$ is a function slowly varying with range and denotes the demodulated outgoing complex-valued envelope function governed by the stochastic PE (Jensen *et al.*, 2011; Lin *et al.*, 2013; Tappert, 1977)

$$\frac{\partial}{\partial\eta}\psi(\boldsymbol{x}_\perp, \eta; \xi) = ik_0\left\{-1 + \sqrt{1 + \frac{1}{k_0^2}\nabla_\perp^2 + n_{eff}^2(\boldsymbol{x}_\perp, \eta; \xi) - 1}\right\} \times \psi(\boldsymbol{x}_\perp, \eta; \xi), \tag{6}$$

where $\boldsymbol{x}_\perp = (x_1, x_2)$ and $\nabla_\perp$ is the 2-D transverse Laplacian operator, defined as

$$\nabla_\perp^2 = \frac{\partial^2}{\partial x_1^2} + \frac{\partial^2}{\partial x_2^2}. \tag{7}$$

With uncertainties in the environment and acoustic parameters, Eq. (6) is a stochastic partial differential equation (SPDE) that can be written in operator form as

$$\frac{\partial\psi(\boldsymbol{x}_\perp, \eta; \xi)}{\partial\eta} = \mathcal{L}_{PE}[\psi(\boldsymbol{x}_\perp, \eta; \xi); \xi], \quad \boldsymbol{x}_\perp \in \mathcal{D},\ \eta \in (0, R],\ \xi \in \Xi, \tag{8}$$

where $\mathcal{L}_{PE}$ is the stochastic PE operator defined as

$$\mathcal{L}_{PE}[\psi(\boldsymbol{x}_\perp, \eta; \xi); \xi] = ik_0\left\{-1 + \sqrt{1 + \frac{1}{k_0^2}\nabla_\perp^2 + n_{eff}^2(\boldsymbol{x}_\perp, \eta; \xi) - 1}\right\} \times \psi(\boldsymbol{x}_\perp, \eta; \xi). \tag{9}$$

Within Eqs. (8) and (9), the sources of stochasticity in the predicted acoustic field $\psi(\boldsymbol{x}_\perp, \eta; \xi)$ are the uncertain sound speed $c(\boldsymbol{x}_\perp, \eta; \xi)$, density $\rho(\boldsymbol{x}_\perp, \eta; \xi)$, and attenuation $a(\boldsymbol{x}_\perp, \eta; \xi)$ fields, and hence the uncertain index of refraction field $n_{eff}(\boldsymbol{x}_\perp, \eta; \xi)$.

As acoustic PEs are of the parabolic type, initial conditions are needed at the starting range $\eta = \eta_s$. Several analytical and numerical starters have been proposed to initialize the deterministic PE including the Gaussian, Greene, and Thomson's sources (Jensen *et al.*, 2011), and the PE self-starter (Collins, 1992, 1999). For example, the deterministic Gaussian source (Tappert, 1977) is defined by $\psi(\boldsymbol{x}_\perp, \eta_s) = \sqrt{k_0}e^{-k_0^2/2(x_1-x_{1,s})^2}e^{-k_0^2/2(x_2-x_{2,s})^2}$, where $\boldsymbol{x}_{\perp,s} = (x_{1,s}, x_{2,s})$ denotes the source location. In this work, such deterministic starters are extended to stochastic starters $\psi(\boldsymbol{x}_\perp, \eta_s(\xi); \xi)$ for stochastic PEs in Eqs. (8) and (9) to account for uncertainties in the source range $\eta_s(\xi)$, location $\boldsymbol{x}_{\perp,s}(\xi)$, and frequency $f(\xi)$.

In addition, stochastic boundary conditions could arise, for instance in the presence of rough or uncertain sea surface or interior boundaries (Colosi, 2016; Morozov and Colosi, 2017; Thorsos *et al.*, 2010), forcing uncertainties in the predicted ψ. More specifically, the stochastic PE in Eqs. (8) and (9) is commonly subject to the following:

- *Pressure-release condition at the uncertain sea surface*: $\psi((\boldsymbol{x}_\perp)_{ss}, \eta; \xi) = 0$, where $(\boldsymbol{x}_\perp)_{ss}(\eta; \xi)$ describes the uncertain, e.g., rough, sea surface.
- *Continuity conditions at uncertain interior boundaries:* continuity of pressure $\psi(\boldsymbol{x}_\perp, \eta; \xi)$ and the normal component of particle velocity $1/i\omega\rho(\nabla_\perp\psi \cdot \hat{\boldsymbol{n}})$ where $\hat{\boldsymbol{n}}$ is the unit vector normal to the uncertain, e.g., rough, interior boundary.
- *Outgoing radiation condition at infinity*: in practice, an artificial absorption layer is introduced to prevent spurious reflections from the truncated domains.

All of these stochastic boundary conditions are linear in ψ.

The goal of this work is to predict the stochastic acoustic field $\psi(\boldsymbol{x}_\perp, \eta; \xi)$ and its PDF field, in an unprecedented accuracy and efficiency, using the derived Dynamically Orthogonal Parabolic Equations (DO-PEs).

III. STOCHASTIC DYNAMICALLY ORTHOGONAL PARABOLIC EQUATIONS

The DO formulation for the stochastic PE in Eqs. (8) and (9) is now derived, followed by its application to the narrow-angle PE. Appropriate stochastic boundary conditions (BCs) and stochastic initial conditions (ICs) are described. Finally, numerical schemes for implementing the resulting range-evolution differential equations, BCs, and ICs are provided.

A. Dynamically orthogonal parabolic equations

Starting from the stochastic PE in Eqs. (8) and (9), the DO decomposition (Feppon and Lermusiaux, 2018a,b; Sapsis and Lermusiaux, 2009, 2012) is employed to derive instantaneously-optimal range-dynamic stochastic reduced-order equations. The DO decomposition ψ_{DO} is a range-dynamic extension of the truncated Karhunen-Loève (K-L) decomposition (Alexanderian, 2015; Le Maître and Knio, 2010; Loeve, 1978) defined as

$$\psi(\boldsymbol{x}_\perp, \eta; \xi) \approx \psi_{DO} = \bar{\psi}(\boldsymbol{x}_\perp, \eta) + \sum_{i=1}^{n_{s,\psi}} \widetilde{\psi}_i(\boldsymbol{x}_\perp, \eta)\alpha_i(\eta; \xi), \quad (10)$$

where $\bar{\psi}(\boldsymbol{x}_\perp, \eta)$ is the statistical mean field (units: Pa), $\widetilde{\psi}_i(\boldsymbol{x}_\perp, \eta)$ are orthonormal modes (non-dimensional) that form a basis for the stochastic subspace of size $n_{s,\psi}$, and $\alpha_i(\eta; \xi)$ are zero-mean stochastic processes (units: Pa). Importantly, none of the terms in the right-hand-side of Eq. (10) are here predefined. Instead, for each term, a new range-dynamic differential equation will be obtained next, directly derived from the governing stochastic PE in Eqs. (8) and (9). The resulting system of equations defines the fundamental DO differential PEs. One of them is a PDE governing the evolution in range of the statistical mean field. Similarly, the DO modal basis is *evolved in range* using PDEs. This is thus very different from Empirical Orthogonal Functions (EOFs), Proper Orthogonal Decomposition (POD), or Principal Component Analysis (PCA) where a predefined, range-independent orthonormal basis is used in the transverse physical space. Analogously, PC-based methods use fixed-in-range polynomial basis functionals in the stochastic space (Khine *et al.*, 2010), while the DO coefficients are *evolved in range* according to stochastic ordinary differential equations (ODEs).

To derive the DO differential equations, the DO decomposition [Eq. (10)] is first inserted in the governing Eq. (8). Using the notation defined in Appendix A, the PDE for the mean field $\bar{\psi}$ is derived by applying the expectation operator to Eq. (8). The $n_{s,\psi}$ stochastic ODEs for the coefficients are obtained by Galerkin projection of Eq. (8) onto the subspace defined by the modes $\widetilde{\psi}_i$, i.e., Eq. (8) is multiplied by each mode i followed by integration in the transverse space $\mathcal{D}$. Analogously, the $n_{s,\psi}$ PDEs for the modes are obtained by marginalization in the stochastic coefficients space, i.e., Eq. (8) is multiplied by each coefficient i followed by averaging in the stochastic space Ξ. The results are differential equations for the mean, modes, and stochastic coefficients

$$\frac{\partial \bar{\psi}(\boldsymbol{x}_\perp, \eta)}{\partial \eta} = \mathbb{E}^\xi[\mathcal{L}_{PE}[\psi(\boldsymbol{x}_\perp, \eta; \xi); \xi]], \quad (11a)$$

$$\frac{\partial \widetilde{\psi}_i(\boldsymbol{x}_\perp, \eta)}{\partial \eta} = \sum_{j=1}^{n_{s,\psi}} C^{-1}_{\alpha_i\alpha_j} \Pi^{\perp}_{\widetilde{\psi}} \mathbb{E}^\xi\left[\mathcal{L}_{PE}[\psi(\boldsymbol{x}_\perp, \eta; \xi); \xi]\alpha_j(\eta; \xi)\right], \quad \forall i = 1, \ldots, n_{s,\psi}, \quad (11b)$$

$$\frac{d\alpha_i(\eta; \xi)}{d\eta} = \langle \mathcal{L}_{PE}[\psi(\boldsymbol{x}_\perp, \eta; \xi); \xi] - \mathbb{E}^\xi[\mathcal{L}_{PE}[\psi(\boldsymbol{x}_\perp, \eta; \xi); \xi]], \widetilde{\psi}_i(\boldsymbol{x}_\perp, \eta)\rangle, \quad \forall i = 1, \ldots, n_{s,\psi}, \quad (11c)$$

where $C_{\alpha_i\alpha_j}$ are range-dependent covariance functions,

$$C_{\alpha_i\alpha_j}(\eta) = \mathbb{E}^\xi\left[\alpha_i(\eta; \xi)\alpha_j(\eta; \xi)\right], \quad (12)$$

and $\Pi^{\perp}_{\widetilde{\psi}}$ is a projection operator onto a space orthogonal to the stochastic subspace,

$$\Pi^{\perp}_{\widetilde{\psi}}[v] = v - \sum_{i=1}^{n_{s,\psi}} \langle v, \widetilde{\psi}_i(\boldsymbol{x}_\perp, \eta)\rangle \widetilde{\psi}_i(\boldsymbol{x}_\perp, \eta), \quad (13)$$

where v is a spatial field in the transverse space.

In deriving the DO equations (11a)–(11c), without loss of generality, a condition of dynamical orthogonality is enforced,

$$\left\langle \frac{\partial \widetilde{\psi}_i(\cdot, \eta)}{\partial \eta}, \widetilde{\psi}_j \right\rangle = 0, \quad \forall i, j = 1, \ldots, n_{s,\psi}, \quad (14)$$

restricting the stochastic subspace to evolve orthogonal to itself. This DO condition is a choice of gauge that eliminates redundant degrees of freedom introduced by having both modes and coefficients vary with range. It is not an approximation. Without this condition, an orthonormal basis $\{\widetilde{\psi}_{i=1,\ldots,n_{s,\psi}}\}$ is defined up to any unitary transform, and therefore a change of the solution ψ_{DO} can be represented by either a change of the coefficients, a change of the modes, or a mix of both. The DO condition simply eliminates this redundancy by constraining the change within the subspace to be realized by a change in the coefficients $\alpha_{i=1,\ldots,n_{s,\psi}}$ only, and the subspace evolution to be realized by a change in the modes $\widetilde{\psi}_{i=1,\ldots,n_{s,\psi}}$ only (Feppon and Lermusiaux, 2018b; Sapsis and Lermusiaux, 2009). The key differences between this gauge DO condition and the adiabatic approximation used in normal mode analysis are further examined in Sec. IV.

B. DO-PEs initial and boundary conditions

1. Stochastic initial conditions

To initialize the DO-PEs [Eq. (11)] at a given range $\eta_s = 0$, the Gaussian source is extended to an analytical stochastic Gaussian DO starter that provides the initial mean $\bar{\psi}(\boldsymbol{x}_\perp, 0)$ and the $n_{s,\psi}$ initial modes $\widetilde{\psi}_i(\boldsymbol{x}_\perp, 0)$ and coefficients $\alpha_i(0; \xi)$. Two cases arise depending on whether the source is uncertain (uncertain frequency or location in the transverse space).

Case 1—Uncertain source frequency or source location. In this case, the reference wavenumber k_0 or source position $\boldsymbol{x}_{\perp,s}$ are stochastic, i.e., $k_0 = k_0(\xi)$ or $\boldsymbol{x}_{\perp,s} = \boldsymbol{x}_{\perp,s}(\xi)$, leading to a stochastic Gaussian starter field,

$$\psi(\boldsymbol{x}_\perp, 0; \xi) = \psi^0(\boldsymbol{x}_\perp; \xi) = \sqrt{k_0(\xi)}\, e^{\left[-k_0(\xi)^2/2\right]\left(x_1 - x_{1,s}(\xi)\right)^2} \times e^{\left[-k_0(\xi)^2/2\right]\left(x_2 - x_{2,s}(\xi)\right)^2}, \quad (15)$$

for which the truncated K-L decomposition can be written as

$$\psi(\boldsymbol{x}_\perp,0;\xi)=\psi^0(\boldsymbol{x}_\perp;\xi)\approx\bar{\psi}^0(\boldsymbol{x}_\perp)+\sum_{i=1}^{n_{s,\psi^0}}\tilde{\psi}_i^0(\boldsymbol{x}_\perp)\alpha_i^0(\xi). \quad (16)$$

Using this decomposition, the subspace dimension $n_{s,\psi}$ is selected as n_{s,ψ^0}, and the mean, modes, and coefficients are initialized as

$$\begin{aligned}&\bar{\psi}(\boldsymbol{x}_\perp,0)=\bar{\psi}^0(\boldsymbol{x}_\perp)\,,\\&\tilde{\psi}_i(\boldsymbol{x}_\perp,0)=\tilde{\psi}_i^0(\boldsymbol{x}_\perp),\quad \forall i=1,\dots,n_{s,\psi}\,,\\&\alpha_i(0;\xi)=\alpha_i^0(\xi),\quad \forall i=1,\dots,n_{s,\psi}.\end{aligned} \quad (17)$$

Case 2—Deterministic source frequency and source location. In this case, the analytical Gaussian starter field is deterministic, i.e., $\psi(\boldsymbol{x}_\perp,0;\xi)=\psi(\boldsymbol{x}_\perp,0)=\psi^0(\boldsymbol{x}_\perp)$, such that the initial mean field is

$$\bar{\psi}(\boldsymbol{x}_\perp,0)=\psi^0(\boldsymbol{x}_\perp). \quad (18)$$

Due to the absence of source uncertainties, the stochastic DO coefficients are initialized to be zero, i.e., $\alpha_i(0;\xi)=0$, $\forall i=1,\dots,n_{s,\psi}$. The modes however can be initialized using any orthonormal basis of size $n_{s,\psi}$. The choice of initial orthonormal basis can be arbitrary because the DO-PEs (11) adapt the modes in range to optimally capture the instantaneous dynamics that evolve the stochastic pressure field during range-marching.

In each of the previous two cases, uncertainties in the environment are felt as soon as the numerical DO equations start marching in range. This is illustrated in Part II (Ali and Lermusiaux, 2024), confirming that the DO-PEs dynamically adapt the DO decomposition.

Finally, it should be noted that similar procedures can be used to build DO stochastic wide-angle starters, self-starters (Collins, 1992, 1999), or modal starters (Jensen *et al.*, 2011).

2. Stochastic boundary conditions

As stated at the end of Sec. II, the BCs for the stochastic PE in Eqs. (8) and (9) in the transverse physical space $\mathcal{D}$ are commonly linear. For the DO-PEs [Eq. (11)], the stochastic BCs are thus also linear, and the mean PDE [Eq. (11a)] and modes PDEs [Eq. (11b)] inherit the same type of BCs as all realizations. The BCs for the mean PDE [Eq. (23a)] are the mean of the BCs. The BCs for the PDE of mode i [Eq. (23b)] are obtained by multiplication of the original BCs by stochastic coefficient i followed by averaging in the stochastic space Ξ. Additional details on more complex BC schemes are provided in Gupta *et al.* (2016).

The stochastic coefficients from Eq. (11c) are ODEs in the independent range variable η, and hence do not require BCs. They only require ICs to march in range as discussed in the previous subsection.

C. DO-PEs properties

First, the governing DO-PE [Eq. (11)] and their ICs and BCs, respect nonlinearities and uncertainties in the original governing stochastic PE [Eq. (8)] and its ICs and BCs. Second, they dynamically adapt in range to the evolving physics and uncertainties. Third, instantaneously in range, the DO-PE equations optimally reduce the original system, as they define and integrate in the tangent space to the nonlinear reduced manifold. They reduce the stochastic PE dynamics by instantaneously taking its singular value decomposition (SVD) and they can be shown to track the best low-rank approximation. These properties are derived and examined in Feppon and Lermusiaux (2018a,b) and further exploited in Charous and Lermusiaux (2023a,c). Fourth, for many ocean acoustic applications, the number $n_{s,\psi}$ of DO modes $\tilde{\psi}_i(\boldsymbol{x}_\perp,\eta)$ needed to represent most of the stochastic field variance (energy) is much smaller than the discrete dimension n_ψ of the stochastic PE [Eq. (8)] spatially-discretized in the transverse directions. This is mainly because of the correlations among nearby ocean acoustics variables. The result is a drastic reduction in computational costs.

Indeed, starting from the original stochastic acoustic PE [Eq. (8)], if the transverse spatial directions are discretized and the scalar stochastic coefficients integrated using an MC scheme, i.e., one ODE for each realization, the DO equations (11a)–(11c)] become a low-rank matrix-ODE in range (Feppon and Lermusiaux, 2018a,b). If the MC scheme uses n_r realizations (ensemble members) and the discretized transverse-space dimension is n_ψ, the DO methodology reduces the $n_r\times n_\psi$ matrix-ODE system to only (i) one discretized PDE of dimension n_ψ for the evolution of the mean [Eq. (11a)], (ii) $n_{s,\psi}$ discretized PDEs of dimension n_ψ for the modes [Eq. (11b)], and (iii) $n_{s,\psi}\times n_r$ discretized ODEs for the stochastic coefficients [Eq. (11c)]. Since $n_{s,\psi}\ll n_\psi$, the range-dynamic reduced-order stochastic DO system is very efficient to solve the stochastic PE [Eq. (8)] in range (Charous and Lermusiaux, 2021; Ueckermann *et al.*, 2013), see Sec. III F.

Fifth, continuing with the discretized matrix-ODE DO system, the DO decomposition [Eq. (10)] at range η, denoted by the matrix Ψ_{DO}, is the rank-$n_{s,\psi}$ approximation of the full rank matrix of realizations Ψ of size $n_r\times n_\psi$, at that same range η. While the truncated SVD is well known to provide the optimal low-rank approximation (in the Frobenius norm and spectral norm or 2-norm), obtaining this low-rank approximation at every range step would require integrating and storing the full matrix of realizations and then performing SVD at every step. In practice, both of these steps become prohibitively expensive. Instead, the DO method allows to optimally and adaptively evolve the system's low-rank approximation Ψ_{DO} in range without the need to compute the full realizations matrix Ψ nor perform its SVD at every range step.

D. Application to the standard narrow-angle parabolic equation

Due to the presence of the pseudo-differential square-root operator in the acoustic PE [Eq. (6)], several PE approximations have been proposed (Jensen *et al.*, 2011). In Part II (Ali and Lermusiaux, 2024), the standard narrow-angle approximation is used. The square-root operator is then approximated using a first-order Taylor series expansion to obtain the stochastic narrow-angle PE (NAPE) (Tappert, 1977),

$$\frac{\partial}{\partial\eta}\psi(\boldsymbol{x}_\perp,\eta;\xi) = \left\{\frac{i}{2k_0}\nabla_\perp^2 + \frac{ik_0}{2}\left(n_{eff}^2(\boldsymbol{x}_\perp,\eta;\xi)-1\right)\right\} \times \psi(\boldsymbol{x}_\perp,\eta;\xi). \tag{19}$$

The stochastic ICs and BCs for Eq. (19) are commonly as those of the stochastic PE in Eqs. (8) and (9).

The DO range-evolution equations for the stochastic NAPE [Eq. (19)] are now obtained. As for the DO-PEs [Eq. (11)], the start is range-dynamic K-L (DO) expansions, here for both the input index of refraction field $n_{eff}^2(\boldsymbol{x}_\perp,\eta;\xi)$ and output complex envelope pressure field $\psi(\boldsymbol{x}_\perp,\eta;\xi)$,

$$n_{eff}^2(\boldsymbol{x}_\perp,\eta;\xi) \approx \left(n_{eff}^2\right)_{DO} = \overline{n^2}(\boldsymbol{x}_\perp,\eta) + \sum_{l=1}^{n_{s,n^2}} \widetilde{n^2}_l(\boldsymbol{x}_\perp,\eta)\beta_l(\eta;\xi), \tag{20a}$$

$$\psi(\boldsymbol{x}_\perp,\eta;\xi) \approx \psi_{DO} = \bar{\psi}(\boldsymbol{x}_\perp,\eta) + \sum_{i=1}^{n_{s,\psi}} \widetilde{\psi}_i(\boldsymbol{x}_\perp,\eta)\alpha_i(\eta;\xi). \tag{20b}$$

In Eq. (20), $\overline{n^2}(\boldsymbol{x}_\perp,\eta)$ and $\bar{\psi}(\boldsymbol{x}_\perp,\eta)$ are statistical mean fields for the index of refraction and complex pressure, respectively. The fields $\widetilde{n^2}_l(\boldsymbol{x}_\perp,\eta)$, $\forall l = 1,\dots,n_{s,n^2}$, and $\widetilde{\psi}_i(\boldsymbol{x}_\perp,\eta)$, $\forall i = 1,\dots,n_{s,\psi}$, are DO modes, each set defining a range-dynamic basis, orthonormal in the transverse spatial space by construction. The DO stochastic coefficients $\beta_l(\eta;\xi)$, $\forall l = 1,\dots,n_{s,n^2}$, and $\alpha_i(\eta;\xi)$, $\forall i = 1,\dots,n_{s,\psi}$, are each zero-mean stochastic processes that can represent complex range-dependent uncertainties in the squared effective index of refraction and acoustic fields, respectively. Since the DO modes are orthonormal by construction, the magnitude of their contribution is determined by the corresponding stochastic coefficient. Again, none of the mean, DO modes, and DO coefficients in the right-hand-sides of Eq. (20b) are predefined but instead are here governed by new differential DO equations derived directly from the governing stochastic NAPE [Eq. (19)]. The only assumption is that the DO expansions $(n_{eff}^2)_{DO}$ in Eq. (20a) and ψ_{DO} in Eq. (20b) are truncated to subspaces of size n_{s,n^2} and $n_{s,\psi}$, respectively, so as to capture most of the stochastic fields n_{eff}^2 and ψ, in the sense of explained variance. The right-hand-side of Eq. (20a) is obtained, for example, from DO ocean equations or a probabilistic modeling system (Lermusiaux, 1999, 2007; Lermusiaux *et al.*, 2020b; Lermusiaux and Robinson, 1999; Lermusiaux *et al.*, 2010; Robinson *et al.*, 2002).

For ease of notation, we omit the independent variables, and rewrite the expansions in Eq. (20) as

$$\left(n_{eff}^2\right)_{DO} = \overline{n^2} + \sum_{l=1}^{n_{s,n^2}} \widetilde{n^2}_l\beta_l, \tag{21a}$$

$$\psi_{DO} = \bar{\psi} + \sum_{i=1}^{n_{s,\psi}} \widetilde{\psi}_i\alpha_i. \tag{21b}$$

Substituting these expansions, Eq. (21) in the stochastic NAPE [Eq. (19)] gives

$$\frac{\partial\bar{\psi}}{\partial\eta} + \sum_{i=1}^{n_{s,\psi}}\alpha_i\frac{\partial\widetilde{\psi}_i}{\partial\eta} + \sum_{i=1}^{n_{s,\psi}}\widetilde{\psi}_i\frac{d\alpha_i}{d\eta} = \left\{\frac{i}{2k_0}\nabla_\perp^2 + \frac{ik_0}{2}\left(\overline{n^2} + \sum_{l=1}^{n_{s,n^2}}\widetilde{n^2}_l\beta_l - 1\right)\right\} \times \left(\bar{\psi} + \sum_{i=1}^{n_{s,\psi}}\widetilde{\psi}_i\alpha_i\right). \tag{22}$$

Starting from Eq. (22), the derivation of the range evolution equations for the mean, modes, and coefficients is provided in Appendix B. The results are the following DO-NAPEs:

$$\frac{\partial\bar{\psi}(\boldsymbol{x}_\perp,\eta)}{\partial\eta} = \frac{i}{2k_0}\nabla_\perp^2\bar{\psi} + \frac{ik_0}{2}\bar{\psi}\left(\overline{n^2}-1\right) + \sum_{i=1}^{n_{s,\psi}}\sum_{l=1}^{n_{s,n^2}}\frac{ik_0}{2}C_{\alpha_i\beta_l}\widetilde{n^2}_l\widetilde{\psi}_i, \tag{23a}$$

$$\frac{\partial\widetilde{\psi}_i(\boldsymbol{x}_\perp,\eta)}{\partial\eta} = Q_i - \sum_{j=1}^{n_{s,\psi}}\langle Q_i,\widetilde{\psi}_j\rangle\widetilde{\psi}_j, \quad \forall i=1,\dots,n_{s,\psi}, \tag{23b}$$

where

$$Q_i = \frac{i}{2k_0}\nabla_\perp^2\widetilde{\psi}_i + \frac{ik_0}{2}(\overline{n^2}-1)\widetilde{\psi}_i + \sum_{n=1}^{n_{s,\psi}}C^{-1}_{\alpha_n\alpha_i}\left[\sum_{l=1}^{n_{s,n^2}}C_{\alpha_n\beta_l}\frac{ik_0}{2}\widetilde{n^2}_l\bar{\psi} + \sum_{k=1}^{n_{s,\psi}}\sum_{l=1}^{n_{s,n^2}}E^{\xi}[\alpha_n\beta_l\alpha_k]\frac{ik_0}{2}\widetilde{n^2}_l\widetilde{\psi}_k\right],$$

$$\frac{d\alpha_i(\eta;\xi)}{d\eta} = \sum_{k=1}^{n_{s,\psi}}\alpha_k\left\langle\frac{i}{2k_0}\nabla_\perp^2\widetilde{\psi}_k,\widetilde{\psi}_i\right\rangle + \sum_{k=1}^{n_{s,\psi}}\alpha_k\left\langle\frac{ik_0}{2}(\overline{n^2}-1)\widetilde{\psi}_k,\widetilde{\psi}_i\right\rangle + \sum_{l=1}^{n_{s,n^2}}\beta_l\left\langle\frac{ik_0}{2}\widetilde{n^2}_l\bar{\psi},\widetilde{\psi}_i\right\rangle + \sum_{k=1}^{n_{s,\psi}}\sum_{l=1}^{n_{s,n^2}}\left(\alpha_k\beta_l - C_{\alpha_k\beta_l}\right)\left\langle\frac{ik_0}{2}\widetilde{n^2}_l\widetilde{\psi}_k,\widetilde{\psi}_i\right\rangle, \quad \forall i=1,\dots,n_{s,\psi}. \tag{23c}$$

In these three sets of equations, C denotes a range-varying covariance matrix between two stochastic processes.

For instance, $C_{\alpha_i\beta_l}(\eta) = E^{\xi}[\alpha_i(\eta;\xi)\beta_l(\eta;\xi)]$. The solution of the DO NAPEs [Eq. (23)] provides predictions of the stochastic acoustic field $\psi(\boldsymbol{x}_\perp, \eta; \xi)$, where $\boldsymbol{x}_\perp \in \mathcal{D}$ and $\eta \in (0, R]$, for all realizations $\xi \in \Xi$.

Similar to the DO-PEs, the DO-NAPEs [Eq. (23)] are subject to the DO stochastic BCs discussed in Sec. III B 2 and are initialized using the ICs described in Sec. III B 1. The numerical schemes used in their implementation are outlined next. For more details on the discrete DO-PEs and DO-NAPEs, we refer to Ali (2023).

E. Numerical schemes

The numerical schemes and implementation of the stochastic DO-NAPEs [Eq. (23)] are presented now. These coupled DO-NAPEs consist of (i) a modified deterministic PE for the mean field, $\bar{\psi}(\boldsymbol{x}_\perp, \eta)$, (ii) $i = 1, \ldots, n_{s,\psi}$ modified deterministic PEs for the DO mode fields, $\tilde{\psi}_i(\boldsymbol{x}_\perp, \eta)$, and (iii) $i = 1, \ldots, n_{s,\psi}$ stochastic ODEs (S-ODEs) for the zero-mean stochastic coefficient processes, $\alpha_i(\eta;\xi)$. The former $n_{s,\psi} + 1$ PEs are PDEs discretized in the transverse physical space $\mathcal{D}$ with range-marching while the latter $n_{s,\psi} + 1$ S-ODEs are discretized in the reduced stochastic space with range-marching.

1. Discretization in the transverse physical space $\mathcal{D}$

For the $n_{s,\psi} + 1$ modified PEs, a finite volume framework (Ueckermann and Lermusiaux, 2012) is used in the physical space $\mathcal{D}$ transverse to the marching direction η. Specifically, a 2nd order central difference scheme is used for the transverse Laplacian operator $\nabla_\perp^2$. Special care is taken to account for the inhomogeneous density in the medium by applying smoothing functions at the water-seabed and each of the sediment interfaces (Jensen *et al.*, 2011; Tappert, 1977). Further details about the discretization schemes can be found in (Ali, 2019; Ali *et al.*, 2019; Ali *et al.*, 2023) where the accuracy of our deterministic PE solver is validated by comparison with reference analytical solutions and with numerical KRAKEN (Porter, 1991, 2010) and RAM (Collins *et al.*, 1996; Porter, 2010) solutions, in both range-independent and range-dependent benchmark problems. The stochastic DO-NAPEs were then implemented based on the same discrete operators indeed, once a deterministic code is available, implementing the additional DO terms and equations can be done by reusing existing codes with minor updates (Subramani and Lermusiaux, 2024).

2. Range marching

For range marching over $\eta \in (0, R]$, a second-order semi-implicit backward differencing (SBDF2) scheme is used to integrate the mean and DO modes PDEs, Eqs. (23a) and (23b). In these PDEs, all linear terms are handled implicitly (i.e., *evaluated* at the current range of interest), while (stochastic) nonlinear terms are handled explicitly (i.e., *evaluated* at previous ranges).

To integrate the stochastic ODEs governing the evolution of the stochastic DO coefficients with range, we use a direct MC method and evolve n_r samples of the $n_{s,\psi}$ coefficients using a second-order explicit backward differencing scheme. Given that the coefficients are governed by stochastic ODEs rather than S-PDEs, the direct MC method is the most straightforward technique without significant computational costs. This is because only $n_{s,\psi}$ scalar coefficients are marched in range, with $n_{s,\psi} \ll n_\psi$, so even when $n_r \sim n_\psi$, the cost of evolving n_r samples for each DO coefficient is not significant compared to the cost of integrating the PDEs for the DO modes and mean fields. Further details can be found in Ali (2019) and Ueckermann *et al.* (2013).

3. Initial condition schemes

A direct stochastic initialization scheme is used to obtain the ICs for the DO-NAPE mean, modes, and coefficients. The two cases outlined in Sec. III B 1 are implemented.

For case 1 with an uncertain source frequency or source location, n_r samples are obtained from the initial frequency and/or location distributions which are then used to build the realizations matrix of the starter field. After that, the SVD of this matrix is obtained and truncated to capture 99% of the variance in the starter realizations. The truncated SVD gives the ICs of the DO-NAPE mean, modes, and coefficients.

For case 2 with a deterministic source frequency and location, the analytical Gaussian starter field is deterministic and thus used to initialize the DO-NAPE mean. The DO-NAPE coefficients are initialized to zero and the DO-NAPE modes to any orthonormal basis of size $n_{s,\psi}$, for instance, the canonical basis of unit vectors. The optimal subspace size $n_{s,\psi}$ can be obtained adaptively or by convergence studies, see Part II (Ali and Lermusiaux, 2024).

Another indirect approach to initialize the DO-NAPE mean, modes, and coefficients consists of running first an ensemble of short-range deterministic NAPE simulations. An ensemble of realizations $\psi(\boldsymbol{x}_\perp, \eta; \xi)$ is then integrated for a few range steps $\eta \in (0, R_i]$, e.g., $R_i = 15 - 20\lambda$, starting from an ensemble of initial source locations, sound speed, density, and/or attenuation fields. A truncated SVD of the ensemble fields at $\eta = R_i$ then yields the initial conditions of the mean, modes, and stochastic coefficients, from which the DO-NAPEs start and evolve the fields to the final range of interest. This approach may be beneficial when comparing the DO-NAPEs solutions to those from an MC ensemble as the correspondence between the MC realizations and the DO-NAPE coefficient realizations is easily maintained at all ranges. However, implementing and then running an ensemble to start the DO equations is more complex than the direct scheme mentioned previously. In addition, if numerical reorthonormalization is employed during the DO integration, appropriate techniques are commonly needed to maintain this one-to-one correspondence, as discussed in Lin and Lermusiaux (2021). More importantly, when the uncertainty dimensions increase, running the short-range MC ensemble becomes expensive or even infeasible. For all these reasons, we found that the direct initialization scheme is preferred.

F. Computational costs

Per range step, the computational cost of solving the deterministic NAPE is dominated by the stiff Laplacian term $(i/2k_0)\nabla_\perp^2\psi(\boldsymbol{x}_\perp,\eta)$ which is typically treated implicitly. This leads to solving a $N_{\boldsymbol{x}_\perp}\times N_{\boldsymbol{x}_\perp}$ linear system where $N_{\boldsymbol{x}_\perp}$ is the number of grid points in the transverse physical space $\mathcal{D}$. The cost of solving this system scales super-linearly as $\mathcal{O}(N_{\boldsymbol{x}_\perp}^\kappa)$, with $1\le\kappa<2$ depending on the dimension of $\mathcal{D}$ and the algorithm used to solve the linear system. For instance, the case of a one-dimensional (1D) transverse physical space ($D\equiv z$) with a 2nd order central differencing scheme gives a tridiagonal linear system whose solution cost scales linearly with the number of grid points, i.e., $\kappa=1$. A direct MC solution with n_r realizations therefore scales as $\mathcal{O}(n_rN_{\boldsymbol{x}_\perp}^\kappa)$. On the other hand, the cost of solving the stochastic DO-NAPEs [Eq. (23)] per range step is dominated by the analogous Laplacian terms $(i/2k_0)\nabla_\perp^2\widetilde{\psi}_i$ (treated implicitly) and the nonlinear projection terms $\left\langle\widetilde{n^2}_l\widetilde{\psi}_k,\widetilde{\psi}_i\right\rangle$ (treated explicitly) in the DO modes equations. Their costs scale as $\mathcal{O}(n_{s,\psi}N_{\boldsymbol{x}_\perp}^\kappa)$ and $\mathcal{O}(n_{s,n^2}n_{s,\psi}^2N_{\boldsymbol{x}_\perp})$, respectively. By leveraging vectorization and highly-optimized subroutines, the cost of the nonlinear projection terms can be scaled down by implementing the projection as a matrix-matrix multiplication to become $\mathcal{O}(n_{s,n^2}n_{s,\psi}N_{\boldsymbol{x}_\perp})$. The total cost of the stochastic DO-NAPEs therefore scales as $\mathcal{O}(n_{s,\psi}N_{\boldsymbol{x}_\perp}^\kappa+n_{s,n^2}n_{s,\psi}N_{\boldsymbol{x}_\perp})$. It should be noted that this cost is independent of the number of realizations n_r which only affects the DO coefficients ODEs. We also note that the cost of inverting the covariance of the coefficients is commonly negligible as it is at most cubic in $n_{s,\psi}$ and usually $\mathcal{O}(n_{s,\psi}^3)\ll\mathcal{O}(n_{s,\psi}N_{\boldsymbol{x}_\perp}^\kappa+n_{s,n^2}n_{s,\psi}N_{\boldsymbol{x}_\perp})$.

Taking the ratio of the MC cost to the DO cost, we thus have

$$\frac{\text{Cost}_{MC}}{\text{Cost}_{DO}}\sim\frac{n_rN_{\boldsymbol{x}_\perp}^{\kappa-1}}{n_{s,\psi}N_{\boldsymbol{x}_\perp}^{\kappa-1}+n_{s,n^2}n_{s,\psi}}. \tag{24}$$

Equation (24) shows that the computational speedup offered by the DO-NAPE can be several orders of magnitude. It commonly increases for higher dimensions and higher-order numerical schemes. Furthermore, for typical ocean acoustic applications, $N_{\boldsymbol{x}_\perp}^{\kappa-1}\gg n_{s,n^2}$, and Eq. (24) reduces to

$$\frac{\text{Cost}_{MC}}{\text{Cost}_{DO}}\rightarrow\frac{n_r}{n_{s,\psi}},$$

which highlights the efficiency of the DO-NAPE in capturing thousands to millions of realizations, a challenging task for MC methods, at a much-reduced computational cost.

In addition to the computational speedup, the DO-NAPEs have a memory storage advantage over direct MC. Specifically, for direct MC, the storage required per range step is $\mathcal{O}(n_rN_{\boldsymbol{x}_\perp})$. For the DO-NAPE mean, modes, and coefficients at each range step, however, the storage required is, $\mathcal{O}(N_{\boldsymbol{x}_\perp})$, $\mathcal{O}(n_{s,\psi}N_{\boldsymbol{x}_\perp})$, and $\mathcal{O}(n_{s,\psi}n_r)$, respectively. The total storage needed for the DO-NAPEs is thus $\mathcal{O}(n_{s,\psi}(n_r+N_{\boldsymbol{x}_\perp}))$ offering memory savings of

$$\frac{\text{Memory}_{MC}}{\text{Memory}_{DO}}\sim\frac{n_rN_{\boldsymbol{x}_\perp}}{n_{s,\psi}(n_r+N_{\boldsymbol{x}_\perp})}. \tag{25}$$

Of course, the exact computational speedup and memory savings depend on the numerical implementation. For instance, the previously-mentioned vectorization used to reduce the computational costs of the nonlinear projection terms $\left\langle\widetilde{n^2}_l\widetilde{\psi}_k,\widetilde{\psi}_i\right\rangle$ may lead to storage requirements of $\mathcal{O}(n_{s,n^2}n_{s,\psi}N_{\boldsymbol{x}_\perp})$ to first store the Hadamard product $\widetilde{n^2}_l\widetilde{\psi}_k$ before using the matrix-matrix multiplication for the projection. This trade-off between computational time and memory storage can be optimized based on the objectives and resource constraints. Considering parallel and distributed computing (Dutt *et al.*, 2018; Evangelinos *et al.*, 2009, 2011), the discrete DO-PEs can be distributed (Subramani and Lermusiaux, 2024), which alters the previously noted cost scaling and reduces the DO-PE computational time. Of course, a brute-force deterministic MC ensemble integration is embarrassingly parallel, but its storage and post-processing costs (statistics, etc.) become prohibitive for realistic acoustics and larger ensemble sizes, e.g., $n_r>\mathcal{O}(10^3)$. As gains are limited by the processors and memory available, it is mostly for smaller ensembles that parallelization can reduce the computational time for MC more than for DO-PE. However, even in these conditions, as the previously noted ratios are not good for MC and as the DO-PEs adapt to dominant uncertainties with range, the efficiency (ratio of accuracy to total cost) often favors the DO-PEs, as highlighted by the applications in Part II (Ali and Lermusiaux, 2024).

G. Postprocessing: TL DO decompositions

Using the numerical schemes discussed previously, the DO-NAPEs [Eq. (23)] are solved for the complex-valued mean field $\bar{\psi}(\boldsymbol{x}_\perp,\eta)$, modes $\widetilde{\psi}_{i=1,\dots,n_{s,\psi}}(\boldsymbol{x}_\perp,\eta)$, and stochastic coefficients $\alpha_{i=1,\dots,n_{s,\psi}}(\eta;\xi)$. Whenever required, the TL solution can be constructed as

$$\begin{aligned}TL(\boldsymbol{x}_\perp,\eta;\xi)&=-20\log_{10}|\psi(\boldsymbol{x}_\perp,\eta;\xi)|\\&=-20\log_{10}|\bar{\psi}+\sum_{i=1}^{n_{s,\psi}}\widetilde{\psi}_i\alpha_i|\ .\end{aligned} \tag{26}$$

The DO decomposition of Eq. (26) can be computed using SVD with two approaches:

(1) *Range-dependent SVD*. Stepping through range, for each $\eta^*\in(0,R]$, the DO decomposition of the stochastic two-dimensional (2D) TL field (at a fixed range η^*, TL is only a function of $\boldsymbol{x}_\perp$) is computed by taking the SVD of the 2D realization fields $TL(\boldsymbol{x}_\perp,\eta^*;\xi)$. These SVDs

taken at each discrete range η^* yield the mean field $\overline{TL}(\boldsymbol{x}_\perp, \eta^*)$ (units: dB), modes $\widetilde{TL}_{k=1,\ldots,n_{s,TL}}(\boldsymbol{x}_\perp, \eta^*)$ (non-dimensional), and stochastic coefficients $\gamma_{k=1,\ldots,n_{s,TL}}(\eta^*; \xi)$ (units: dB).

(2) *Global SVD*. At the end of range marching, the DO decomposition of the stochastic 3D TL field is computed in one shot, for all ranges at once, by taking the SVD of the 3D realization fields $TL(\boldsymbol{x}_\perp, \eta; \xi)$. The mean field $\overline{TL}(\boldsymbol{x}_\perp, \eta)$ (units: dB), modes $\widetilde{TL}_{k=1,\ldots,n_{s,TL}}(\boldsymbol{x}_\perp, \eta)$ (non-dimensional), and stochastic coefficients $\gamma_{k=1,\ldots,n_{s,TL}}(\xi)$ (units: dB) are obtained. Note that the DO coefficients of the 3D TL in this approach are then global and thus range-independent.

In both approaches, the number of modes retained in the truncated SVD is denoted as $n_{s,TL}$. It is the rank of the approximating matrix and of the DO decomposition for TL, and is chosen to capture the dominant TL uncertainties by thresholding the corresponding singular values. Note that both approaches post-process the DO decomposition of the stochastic acoustic field $\psi(\boldsymbol{x}_\perp, \eta; \xi)$ to obtain a decomposition for TL.

IV. DIFFERENCES FROM ADIABATIC AND COUPLED NORMAL MODES

Although both the DO-PEs and acoustic normal modes theories are based on modal expansions, they exhibit fundamental differences in their underlying principles, mathematical frameworks, and physics explained. These differences are summarized as follows:

(1) Mathematical Framework:

- DO-PEs: As shown in Sec. III, the DO-PEs here decompose all the stochastic fields in the governing *stochastic Parabolic Equation* in terms of their dynamic K-L (DO) expansions into statistical means, orthonormal stochastic subspace modes, and stochastic coefficients, and then obtain differential equations for each by applying expectation and projection operators. The results are governing DO-PEs, see Eqs. (11) and (23), for the mean, DO modes, and stochastic coefficients that are marched in range to obtain the stochastic envelope pressure field ψ. Importantly, none of the mean, DO modes, and DO coefficients, are predefined. Instead, they are governed by the stochastic DO-PEs directly derived from the stochastic PE and adapt in range to the dominant uncertainties. The only assumption made in the DO-PEs is when the dynamic K-L is truncated, leading to a reduced-order DO-PE system and stochastic solution ψ. The DO-PEs then define the instantaneously optimal low-rank approximation of the matrix of all the realizations of ψ. These properties are illustrated in Part II (Ali and Lermusiaux, 2024).
- Normal Modes: On the other hand, normal mode analysis is originally based on expanding the solution of the *deterministic, commonly Helmholtz equation* (i.e., where the environment and acoustic parameters are exactly known) in terms of the coupled waveguide eigenmodes (Jensen *et al.*, 2011; Pekeris, 1948). This is followed by subdividing the propagation range into a sequence of range-independent segments within which an eigenvalue problem is solved for the local eigenmodes. The eigenvalue problem has an infinite number of eigenmodes. In practice, only the maximum number of physically meaningful eigenmodes is retained (e.g., only lossless modes if interested in the far-field solution) and form an orthonormal basis. Furthermore, the modal coefficients are obtained by imposing continuity conditions at the interface of successive range segments and Galerkin projection onto the basis of the new range segment (Evans, 1983). This approach, however, can become computationally intensive. Two main simplifications have been proposed: (1) one-way coupled modes (McDaniel, 1982), and (2) the adiabatic approximation (Pierce, 1965).

(2) Physical Interpretation of the Modes:

- DO-PEs: The DO-PEs organize and track uncertainty according to variance, integrating in range the local sources of uncertainty with the spread of acoustic propagation dynamics. They evolve and organize the dominant modes of stochastic variability in the acoustic field. The individual DO modes thus represent a combination of acoustic processes and environmental influences, combining contributions from the uncertain source, reflections, refractions, and other complex interactions. The modes may not correspond to specific acoustic phenomena in a straightforward manner, but they optimally capture the significant (in the sense of explained variance) transverse spatial patterns in the propagating stochastic acoustic field.
- Normal Modes: In contrast, normal modes have a clear physical interpretation and represent the resonant behavior of the ocean environment. Each normal mode corresponds to a distinct frequency and associated mode shape, which indicates areas of constructive and destructive interference in the medium (Jensen *et al.*, 2011). They provide insights into phenomena such as wave propagation along specific paths, confinement within waveguides, and interaction with boundaries. As a result, normal modes are sensitive to changes in the ocean environment whereby even slight perturbations (e.g., due to temperature and/or salinity fluctuations) can cause shifts in modal frequencies, alterations in energy distribution, or changes in the number and distribution of nodes and antinodes (Colosi, 2016).

In addition to these differences, it is crucial to highlight key distinctions between the adiabatic approximation (Pierce, 1965) and the DO condition [Eq. (14)]. In the adiabatic approximation, the coupling terms in the normal mode amplitude equations are assumed insignificant and neglected. However, as mentioned in Sec. III A, the DO condition [Eq. (14)] is simply a gauge condition that eliminates redundant degrees of freedom introduced by allowing both DO modes and coefficients to vary with range. Therefore, the DO condition does not introduce any new errors. This is highlighted in the DO coefficients governing Eqs. (11c) and (23c) by the mode-coupling terms on their right-hand side. The approximation in the DO-PEs is only due to the truncation of the DO basis to the dominant modes. Most importantly, the DO solution is however allowed to evolve outside the space spanned by the DO modes at a particular range, due to uncertainties in the environment and acoustics in the orthogonal complement of the DO subspace [Eq. (13)]. This evolution of the DO subspace, realized by coupled dynamics outside of the subspace, is governed by [Eq. (11b)]. These DO coupling properties are illustrated in Part II (Ali and Lermusiaux, 2024).

Finally, it is useful to note that the DO decomposition can be used to reduce deterministic acoustics dynamics (Charous and Lermusiaux, 2021, 2023b; Feppon and Lermusiaux, 2018a,b) and has links to dynamical low-rank approximations (Charous and Lermusiaux, 2023a; Koch and Lubich, 2007). Similarly, mode analysis has been usefully extended to handle uncertainties in the ocean environment in the context of random media propagation. This approach, called transport theory (Colosi, 2016; Colosi *et al.*, 1994; Dozier and Tappert, 1978a), relies on first computing the eigenmodes using the deterministic (i.e., unperturbed) environment. Therefore, all the variability due to the uncertainties in the environment is captured by the modal amplitudes. Using the one-way coupled modes assumption, stochastic ordinary differential equations are derived for these modal amplitudes from which moments of the quantities of interest are calculated (Colosi, 2016), usually up to second-order moments, e.g., pressure mean/variance, intensity mean/variance, and mutual coherence functions. Transport theory has been successfully applied in several idealized and realistic ocean cases showing good agreements with observations. However, some stochastic limitations can arise, first due to the use of a predetermined deterministic normal mode basis. This becomes an issue when the true stochastic solution has components outside the space spanned by this predetermined modal basis, either initially or as it advances in range due to environmental uncertainties. In this case, the DO-PEs and the dynamic DO basis would adapt to uncertainties as the solution is marched in range. Second, the DO-PEs theory provides the full PDFs of the stochastic pressure field. It could thus be used to drastically enrich the transport theory approach by capturing PDFs instead of mostly first and second-order moments.

V. SUMMARY AND CONCLUSIONS

In this work, the stochastic DO acoustic PE methodology was developed to model underwater acoustic propagation in uncertain environments. The resulting probabilistic theory and schemes provide an instantaneously optimal range-dynamic model-order reduction technique that evolves the stochastic acoustic field in a range-dynamic subspace. The DO-PEs allow comprehensive and accurate stochastic acoustic modeling at reduced computational costs. Differences between the DO-PE theory and the adiabatic and coupled normal modes theories were also discussed, highlighting distinctions in their underlying principles and mathematical frameworks. The DO-PE methodology was developed for range-dependent environments and applied to the NAPE. The numerical schemes employed for the new DO-NAPEs were described and implemented within a state-of-the-art finite-volume framework.

Since the developed DO equations methodology is not limited to the NAPE formulation, direct extensions of this work include the use of DO for WAPE (Jensen *et al.*, 2011; Lin *et al.*, 2013; Sturm and Fawcett, 2003) and is the subject of a follow-up paper. This allows modeling propagation off the range marching direction with higher accuracy. In addition, the use of the DO equations for 3D stochastic acoustics would offer additional opportunities. Further investigation of the numerical schemes and implementation of the developed DO methodology for memory efficiency and speed may then be useful. Additional extensions of the DO framework in ocean acoustics may include applications for stochastic predictions using ray tracing (Humara *et al.*, 2022) and the acoustic wave equation (Charous and Lermusiaux, 2021), or for efficient solutions of the 3D deterministic NAPE (Charous and Lermusiaux, 2021, 2023b). In Part II (Ali and Lermusiaux, 2024), we evaluate the performance of the DO-NAPEs when applied to three new stochastic range-independent and range-dependent test cases with uncertain sound speed field, bathymetry, and source location. Applications within realistic ocean conditions (Ali, 2023; Ali *et al.*, 2023) are being completed.

The DO-PE methodology can also be used within coupled Bayesian data assimilation where ocean and acoustic data are assimilated to correct predictions and PDFs of ocean physics and acoustics, possibly including seabed properties (Ali *et al.*, 2019). The advantages over standard acoustic inversions such as tomography (Cornuelle *et al.*, 2008; Munk and Wunsch, 1979) and matched field processing (Dosso, 2002; Tolstoy, 1993) include the coupled multivariate estimation (Elisseeff *et al.*, 2002; Lermusiaux and Chiu, 2002) and principled use of non-Gaussian statistics, for example using the Gaussian Mixture Model (GMM) DO filter (Sondergaard and Lermusiaux, 2013a,b) and smoother (Lolla and Lermusiaux, 2017a,b). Additional possibilities include Bayesian acoustic model learning (Gupta and Lermusiaux, 2023; Lu and Lermusiaux, 2021), moving source tomography (Gemba *et al.*, 2022), and adaptive sampling for optimal observations (Wang *et al.*, 2009; Yilmaz *et al.*, 2006).

ACKNOWLEDGMENTS

We thank the members of our MSEAS group. We are grateful to the Office of Naval Research for research support under grants N00014-19-1-2664 (Task Force Ocean: DEEP-AI) and N00014-19-1-2693 (IN-BDA) to the Massachusetts

Institute of Technology. We thank the editor and the reviewers for their useful comments.

AUTHOR DECLARATIONS

Conflict of Interest

The authors have no conflict to disclose.

DATA AVAILABILITY

The data that support the findings of this study are available from the corresponding author upon reasonable request.

APPENDIX A: DO-PE NOTATION

The DO-PEs derived in this paper use the following notation:

- The probability space is defined as $(\Xi, \mathcal{F}, \mu)$ where Ξ is a measurable sample space equipped with an appropriate σ-algebra $\mathcal{F}$ and probability measure μ.
- The mean value (expectation) for a stochastic field $\psi(\boldsymbol{x}_\perp, \eta; \xi)$ is then defined as

$$\bar{\psi}(\boldsymbol{x}_\perp, \eta) = \mathbb{E}^\xi[\psi(\boldsymbol{x}_\perp, \eta; \xi)] = \int_\Xi \psi(\boldsymbol{x}_\perp, \eta; \xi) d\mu(\xi). \quad \text{(A1)}$$

- The spatial transverse inner product, i.e. the inner product in the deterministic physical cross-range domain $\mathcal{D}$, between two (complex-valued) stochastic fields $\psi(\boldsymbol{x}_\perp, \eta; \xi)$ and $\phi(\boldsymbol{x}_\perp, \eta; \xi)$ is defined as

$$\Big\langle \psi(\cdot, \eta; \xi), \phi(\cdot, \eta; \xi) \Big\rangle = \int_\mathcal{D} \psi(\boldsymbol{x}_\perp, \eta; \xi)^* \phi(\boldsymbol{x}_\perp, \eta; \xi) d\boldsymbol{x}_\perp \,, \quad \text{(A2)}$$

  where $*$ denotes the complex conjugate.
- The notations $\bar{\bullet}$ and $\tilde{\bullet}$ denote the statistical mean and dynamically orthonormal modes of $\bullet$, respectively. In particular, $\overline{n^2}(\boldsymbol{x}_\perp, \eta)$ and $\bar{\psi}(\boldsymbol{x}_\perp, \eta)$ are statistical mean fields for the index of refraction and complex pressure, respectively. The fields $\widetilde{n^2}_l(\boldsymbol{x}_\perp, \eta), \forall l = 1, \ldots, n_{s,n^2}$, and $\tilde{\psi}_i(\boldsymbol{x}_\perp, \eta), \forall i = 1, \ldots, n_{s,\psi}$, are DO modes, each set defining a range-dynamic basis, orthonormal in the transverse spatial space. The DO stochastic coefficients $\beta_l(\eta; \xi), l = 1, \ldots, n_{s,n^2}$, and $\alpha_i(\eta; \xi), i = 1, \ldots, n_{s,\psi}$, are each scalar zero-mean stochastic processes that can represent complex range-dependent uncertainties in the squared effective index of refraction and acoustic fields, respectively.

APPENDIX B: DO-NAPE EQUATIONS DERIVATION

The DO-NAPE differential equations are derived directly from the stochastic NAPE [Eq. (19)]. Their solution is the sought-after DO expansion for the complex envelope pressure ψ fields [Eq. (20b)], given the DO expansion for the squared effective index of refraction n^2_{eff} [Eq. (20a)] (e.g., predicted by an ocean model). The exact set of differential equations governing the range evolution of each term in [Eq. (20b)]—i.e., the statistical mean, deterministic DO modes, and zero-mean DO stochastic coefficients—is derived by first substituting the DO decompositions [Eq. (21)] into Eq. (19) to obtain (using Einstein summation notation),

$$\begin{aligned}\frac{\partial \bar{\psi}}{\partial \eta} + \alpha_k \frac{\partial \tilde{\psi}_k}{\partial \eta} + \tilde{\psi}_k \frac{d\alpha_k}{d\eta} &= \frac{i}{2k_0} \nabla^2_\perp \left(\bar{\psi} + \alpha_k \tilde{\psi}_k \right) \\ &\quad + \frac{ik_0}{2} \left(\overline{n^2} + \widetilde{n^2}_l \beta_l - 1 \right) \left(\bar{\psi} + \tilde{\psi}_k \alpha_k \right).\end{aligned}$$

The right-hand side can then be expanded to obtain

$$\begin{aligned}\frac{\partial \bar{\psi}}{\partial \eta} + \alpha_k \frac{\partial \tilde{\psi}_k}{\partial \eta} + \tilde{\psi}_k \frac{d\alpha_k}{d\eta} &= \frac{i}{2k_0} \left[\nabla^2_\perp \bar{\psi} + \alpha_k \nabla^2_\perp \tilde{\psi}_k \right] \\ &\quad + \frac{ik_0}{2} \Big[(\overline{n^2} - 1)\bar{\psi} + (\overline{n^2} - 1)\tilde{\psi}_k \alpha_k \\ &\quad + \widetilde{n^2}_l \beta_l \bar{\psi} + \widetilde{n^2}_l \beta_l \tilde{\psi}_k \alpha_k \Big]. \end{aligned} \quad \text{(B1)}$$

Since both the modes and stochastic coefficients are functions of range, without any loss of generality, a range-dynamical orthonormality condition,

$$\left\langle \frac{\partial \tilde{\psi}_i(\cdot, \eta)}{\partial \eta}, \tilde{\psi}_j \right\rangle = 0\,, \quad \forall i, j = 1, \ldots, n_{s,\psi}, \quad \text{(B2)}$$

is used to resolve the redundancy in the DO representation. This DO condition is simply a gauge that does not introduce new errors but usefully eliminates redundant terms in the equations.

Using Eqs. (B1) and (B2), the range evolution equations for the mean $\bar{\psi}$, modes $\tilde{\psi}_{i=1,\ldots,n_{s,\psi}}$, and stochastic coefficients $\alpha_{i=1,\ldots,n_{s,\psi}}$ are obtained by applying the expectation and inner product operators as shown next.

1. Mean

Applying the expectation operator to both sides of Eq. (B1) gives the mean evolution equation:

$$\frac{\partial \bar{\psi}}{\partial \eta} = \frac{i}{2k_0} \nabla^2_\perp \bar{\psi} + \frac{ik_0}{2} \bar{\psi} (\overline{n^2} - 1) + \frac{ik_0}{2} C_{\alpha_k \beta_l} \widetilde{n^2}_l \tilde{\psi}_k \,, \quad \text{(B3)}$$

where the zero-mean property of the stochastic coefficients was used, i.e., $E^\xi[\alpha_k] = E^\xi[\beta_l] = 0$, for $k = 1, \ldots, n_{s,\psi}$ and $l = 1, \ldots, n_{s,n^2}$, and where $C_{\alpha_k \beta_l} = E^\xi[\alpha_k \beta_l]$ is an element of the acoustic-environment covariance matrix in the stochastic subspace.

2. Coefficients

To obtain the evolution equation for the coefficients α_i, the idea is to eliminate all range-derivatives in (B1) but that of α_i, in other words to isolate $d\alpha_i/d\eta$ on the left-hand side of Eq. (B1). To do so, a Galerkin projection of Eq. (B1) onto the modes $\widetilde{\psi}_i$ is completed, i.e., the inner product of Eq. (B1) with $\widetilde{\psi}_i$ is taken, and then the DO condition [Eq. (B2)] and orthonormality of the modes are used. The result yields the governing equations for the coefficients α_i,

$$\frac{d\alpha_i}{d\eta} = \alpha_k\left\langle \frac{i}{2k_0}\nabla_\perp^2\widetilde{\psi}_k, \widetilde{\psi}_i\right\rangle + \alpha_k\left\langle \frac{ik_0}{2}(\overline{n^2}-1)\widetilde{\psi}_k, \widetilde{\psi}_i\right\rangle + \beta_l\left\langle \frac{ik_0}{2}\widetilde{n^2}_l\bar{\psi}, \widetilde{\psi}_i\right\rangle + \left(\alpha_k\beta_l - C_{\alpha_k\beta_l}\right)\left\langle \frac{ik_0}{2}\widetilde{n^2}_l\widetilde{\psi}_k, \widetilde{\psi}_i\right\rangle,$$
$$\forall i = 1,\ldots,n_{s,\psi}. \tag{B4}$$

3. Modes

To obtain the evolution equation for the modes, the idea is to eliminate all range-derivatives in Eq. (B1) but that of $\widetilde{\psi}_i$, in other words to isolate $\partial\widetilde{\psi}_i/\partial\eta$ on the left-hand side of Eq. (B1). This is done by projection onto the space of stochastic coefficients by first multiplying Eq. (B1) by α_n and then by applying the expectation operator. Using the zero-mean property of α_n (i.e., $E^\xi[\alpha_n]=0$), then yields

$$C_{\alpha_n\alpha_k}\frac{\partial\widetilde{\psi}_k}{\partial\eta} + E^\xi\left[\alpha_n\frac{d\alpha_k}{d\eta}\right]\widetilde{\psi}_k = C_{\alpha_n\alpha_k}\left[\frac{i}{2k_0}\nabla_\perp^2\widetilde{\psi}_k + \frac{ik_0}{2}(\overline{n^2}-1)\widetilde{\psi}_k\right] + C_{\alpha_n\beta_l}\frac{ik_0}{2}\widetilde{n^2}_l\bar{\psi} + E^\xi[\alpha_n\beta_l\alpha_k]\frac{ik_0}{2}\widetilde{n^2}_l\widetilde{\psi}_k. \tag{B5}$$

Using the coefficients Eq. (B4), an expression for $E^\xi[\alpha_n(d\alpha_k/d\eta)]$ can be obtained as

$$E^\xi\left[\alpha_n\frac{d\alpha_k}{d\eta}\right] = C_{\alpha_n\alpha_m}\left\langle \frac{i}{2k_0}\nabla_\perp^2\widetilde{\psi}_m, \widetilde{\psi}_k\right\rangle + C_{\alpha_n\alpha_m}\left\langle \frac{ik_0}{2}(\overline{n^2}-1)\widetilde{\psi}_m, \widetilde{\psi}_k\right\rangle + C_{\alpha_n\beta_l}\left\langle \frac{ik_0}{2}\widetilde{n^2}_l\bar{\psi}, \widetilde{\psi}_k\right\rangle + C_{\alpha_n\alpha_m\beta_l}\left\langle \frac{ik_0}{2}\widetilde{n^2}_l\widetilde{\psi}_m, \widetilde{\psi}_k\right\rangle,$$
$$\forall n,k = 1,\ldots,n_{s,\psi}. \tag{B6}$$

Substituting this expression back into Eq. (B5), exchanging the m and k dummy summation indices to avoid ambiguities, and collecting the terms with the same moment coefficients on the right hand-side yields

$$C_{\alpha_n\alpha_k}\frac{\partial\widetilde{\psi}_k}{\partial\eta} = C_{\alpha_n\alpha_k}\left[\frac{i}{2k_0}\nabla_\perp^2\widetilde{\psi}_k - \left\langle\frac{i}{2k_0}\nabla_\perp^2\widetilde{\psi}_k,\widetilde{\psi}_m\right\rangle\widetilde{\psi}_m\right] + C_{\alpha_n\alpha_k}\left[\frac{ik_0}{2}(\overline{n^2}-1)\widetilde{\psi}_k - \left\langle\frac{ik_0}{2}(\overline{n^2}-1)\widetilde{\psi}_k,\widetilde{\psi}_m\right\rangle\widetilde{\psi}_m\right] + C_{\alpha_n\beta_l}\left[\frac{ik_0}{2}\widetilde{n^2}_l\bar{\psi} - \left\langle\frac{ik_0}{2}\widetilde{n^2}_l\bar{\psi},\widetilde{\psi}_m\right\rangle\widetilde{\psi}_m\right] + E^\xi[\alpha_n\beta_l\alpha_k]\left[\frac{ik_0}{2}\widetilde{n^2}_l\widetilde{\psi}_k - \left\langle\frac{ik_0}{2}\widetilde{n^2}_l\widetilde{\psi}_k,\widetilde{\psi}_m\right\rangle\widetilde{\psi}_m\right],$$
$$\forall n = 1,\ldots,n_{s,\psi}. \tag{B7}$$

This system of equations for the modes evolution can be further simplified by multiplying by the matrix inverse $C^{-1}_{\alpha_n\alpha_k}$ of the symmetric covariance matrix $(C_{\alpha_n\alpha_k})_{1\le n,k\le n_{s,\psi}}$ which yields

$$\frac{\partial\widetilde{\psi}_k}{\partial\eta} = \left[\frac{i}{2k_0}\nabla_\perp^2\widetilde{\psi}_k - \left\langle\frac{i}{2k_0}\nabla_\perp^2\widetilde{\psi}_k,\widetilde{\psi}_m\right\rangle\widetilde{\psi}_m\right] + \left[\frac{ik_0}{2}(\overline{n^2}-1)\widetilde{\psi}_k - \left\langle\frac{ik_0}{2}(\overline{n^2}-1)\widetilde{\psi}_k,\widetilde{\psi}_m\right\rangle\widetilde{\psi}_m\right] + C^{-1}_{\alpha_n\alpha_k}C_{\alpha_n\beta_l}\left[\frac{ik_0}{2}\widetilde{n^2}_l\bar{\psi} - \left\langle\frac{ik_0}{2}\widetilde{n^2}_l\bar{\psi},\widetilde{\psi}_m\right\rangle\widetilde{\psi}_m\right] + C^{-1}_{\alpha_n\alpha_k}E^\xi[\alpha_n\beta_l\alpha_k]\left[\frac{ik_0}{2}\widetilde{n^2}_l\widetilde{\psi}_k - \left\langle\frac{ik_0}{2}\widetilde{n^2}_l\widetilde{\psi}_k,\widetilde{\psi}_m\right\rangle\widetilde{\psi}_m\right],$$
$$\forall k = 1,\ldots,n_{s,\psi}. \tag{B8}$$

To be consistent with Eq. (23b), the indices i and j are used instead of k and m, respectively. The governing evolution equations for the modes are then

$$\frac{\partial\widetilde{\psi}_i}{\partial\eta} = Q_i - \left\langle Q_i,\widetilde{\psi}_j\right\rangle\widetilde{\psi}_j, \quad \forall i = 1,\ldots,n_{s,\psi},$$

where

$$Q_i = \frac{i}{2k_0}\nabla_\perp^2\widetilde{\psi}_i + \frac{ik_0}{2}(\overline{n^2}-1)\widetilde{\psi}_i + C^{-1}_{\alpha_n\alpha_i}\left[C_{\alpha_n\beta_l}\frac{ik_0}{2}\widetilde{n^2}_l\bar{\psi} + E^\xi[\alpha_n\beta_l\alpha_k]\frac{ik_0}{2}\widetilde{n^2}_l\widetilde{\psi}_k\right]. \tag{B9}$$

Akyildiz, I. F., Pompili, D., and Melodia, T. (**2005**). "Underwater acoustic sensor networks: Research challenges," Ad Hoc Networks **3**(3), 257–279.

Alexanderian, A. (**2015**). "A brief note on the Karhunen-Loève expansion," arXiv:1509.07526.

Ali, W. H. (**2019**). "Dynamically orthogonal equations for stochastic underwater sound propagation," Master's thesis, Massachusetts Institute of Technology, Cambridge, MA.

Ali, W. H. (**2023**). "Stochastic dynamically orthogonal modeling and Bayesian learning for underwater acoustic propagation," Ph.D. thesis, Massachusetts Institute of Technology, Cambridge, MA.

Ali, W. H., Bhabra, M. S., Lermusiaux, P. F. J., March, A., Edwards, J. R., Rimpau, K., and Ryu, P. (**2019**). "Stochastic oceanographic-acoustic prediction and Bayesian inversion for wide area ocean floor mapping," in *Proceeding Oceans 2019 MTS/IEEE Seattle*, October 27–31, Seattle, WA, pp. 1–10.

Ali, W. H., Charous, A., Mirabito, C., Haley, P. J., Jr., and Lermusiaux, P. F. J. (**2023**). "MSEAS-ParEq for ocean-acoustic modeling around the globe," in *Proceedings of OCEANS 2023 IEEE/MTS Gulf Coast*, June 5–8, Limerick, Ireland.

Ali, W. H., and Lermusiaux, P. F. J. (**2024**). "Dynamically orthogonal narrow-angle parabolic equations for stochastic underwater sound propagation. Part II: Applications," J. Acoust. Soc. Am. **155**(1), 656–672.
Baggeroer, A. B., Kuperman, W. A., and Mikhalevsky, P. N. (**1993**). "An overview of matched field methods in ocean acoustics," IEEE J. Oceanic Eng. **18**(4), 401–424.
Becker, J., Sandwell, D., Smith, W., Braud, J., Binder, B., Depner, J., Fabre, D., Factor, J., Ingalls, S., Kim, S., Ladner, K., Marks, K., Nelson, S., Pharaoh, A., Trimmer, R., Von Rosenberg, J., Wallace, G., and Weatherall, P. (**2009**). "Global bathymetry and elevation data at 30 arc seconds resolution: SRTM30_PLUS," Mar. Geodesy **32**(4), 355–371.
Benjamin, M. R., Schmidt, H., Newman, P. M., and Leonard, J. J. (**2010**). "Nested autonomy for unmanned marine vehicles with MOOS-IvP," J. Field Rob. **27**(6), 834–875.
Bergmann, P. G. (**1946**). "The wave equation in a medium with a variable index of refraction," J. Acoust. Soc. Am. **17**(4), 329–333.
Bianco, M. J., Gerstoft, P., Traer, J., Ozanich, E., Roch, M. A., Gannot, S., and Deledalle, C.-A. (**2019**). "Machine learning in acoustics: Theory and applications," J. Acoust. Soc. Am. **146**(5), 3590–3628.
Blondel, P. (**2010**). *The Handbook of Sidescan Sonar* (Springer Science & Business Media, New York).
Bonnel, J., Thode, A. M., Blackwell, S. B., Kim, K., and Michael Macrander, A. (**2014**). "Range estimation of bowhead whale (*Balaena mysticetus*) calls in the arctic using a single hydrophone," J. Acoust. Soc. Am. **136**(1), 145–155.
Born, M., Wolf, E., Bhatia, A. B., Clemmow, P. C., Gabor, D., Stokes, A. R., Taylor, A. M., Wayman, P. A., and Wilcock, W. L. (**1999**). "Principles of optics: Electromagnetic theory of propagation," in *Interference and Diffraction of Light*, 7th ed. (Cambridge University Press, Cambridge, UK).
Botseas, G., Lee, D., and King, D. (**1987**). "FOR3D: A computer model for solving the LSS three-dimensional wide angle wave equation," U.S. Naval Underwater Systems Center TR 7943 (Naval Underwater System Center, Newport, RI).
Branicki, M., and Majda, A. J. (**2013**). "Fundamental limitations of polynomial chaos for uncertainty quantification in systems with intermittent instabilities," Commun. Math. Sci. **11**(1), 55–103.
Brekhovskikh, L. M., and Lysanov, Y. (**1982**). *Fundamentals of Ocean Acoustics* (Springer, New York).
Charous, A., and Lermusiaux, P. F. J. (**2021**). "Dynamically orthogonal differential equations for stochastic and deterministic reduced-order modeling of ocean acoustic wave propagation," in *Proceedings of Oceans 2021 IEEE/MTS*, September 20–23, San Diego, CA, pp. 1–7.
Charous, A., and Lermusiaux, P. F. J. (**2023a**). "Dynamically orthogonal Runge–Kutta schemes with perturbative retractions for the dynamical low-rank approximation," SIAM J. Sci. Comput. **45**(2), A872–A897.
Charous, A., and Lermusiaux, P. F. J. (**2023b**). "Range-dynamical low-rank split-step Fourier method for the parabolic wave equation," in preparation.
Charous, A., and Lermusiaux, P. F. J. (**2023c**). "Stable rank-adaptive dynamically orthogonal Runge–Kutta schemes," SIAM J. Sci. Comput. arXiv:2211.07852 (in press).
Chernov, L. A. (**2017**). *Wave Propagation in a Random Medium* (Courier Dover Publications, New York).
Collins, M. D. (**1992**). "A self–starter for the parabolic equation method," J. Acoust. Soc. Am. **92**(4), 2069–2074.
Collins, M. D. (**1995**). "User's guide for RAM versions 1.0 and 1.0 p," Naval Research Lab, Washington, DC.
Collins, M. D. (**1999**). "The stabilized self-starter," J. Acoust. Soc. Am. **106**(4), 1724–1726.
Collins, M. D., Cederberg, R. J., King, D. B., and Chin–Bing, S. A. (**1996**). "Comparison of algorithms for solving parabolic wave equations," J. Acoust. Soc. Am. **100**(1), 178–182.
Colosi, J. A. (**2008**). "Acoustic mode coupling induced by shallow water nonlinear internal waves: Sensitivity to environmental conditions and space-time scales of internal waves," J. Acoust. Soc. Am. **124**(3), 1452–1464.
Colosi, J. A. (**2016**). *Sound Propagation through the Stochastic Ocean* (Cambridge University Press, Cambridge, UK).
Colosi, J. A., Chandrayadula, T. K., Voronovich, A. G., and Ostashev, V. E. (**2013**). "Coupled mode transport theory for sound transmission through an ocean with random sound speed perturbations: Coherence in deep water environments," J. Acoust. Soc. Am. **134**(4), 3119–3133.
Colosi, J. A., Flatté, S. M., and Bracher, C. (**1994**). "Internal–wave effects on 1000-km oceanic acoustic pulse propagation: Simulation and comparison with experiment," J. Acoust. Soc. Am. **96**(1), 452–468.
Cornuelle, B. D., Worcester, P. F., and Dzieciuch, M. A. (**2008**). "Ocean acoustic tomography," J. Phys. **118**, 012002.
Creamer, D. B. (**1996**). "Scintillating shallow-water waveguides," J. Acoust. Soc. Am. **99**(5), 2825–2838.
Creamer, D. B. (**2006**). "On using polynomial chaos for modeling uncertainty in acoustic propagation," J. Acoust. Soc. Am. **119**(4), 1979–1994.
Dashen, R. (**1979**). "Path integrals for waves in random media," J. Math. Phys. **20**(5), 894–920.
Doostan, A., Ghanem, R. G., and Red-Horse, J. (**2007**). "Stochastic model reduction for chaos representations," Comput. Methods Appl. Mech. Eng. **196**(37–40), 3951–3966.
Dosso, S. E. (**2002**). "Quantifying uncertainty in geoacoustic inversion. I. A. fast Gibbs sampler approach," J. Acoust. Soc. Am. **111**(1), 129–142.
Dosso, S. E., Dettmer, J., Steininger, G., and Holland, C. W. (**2014**). "Efficient trans-dimensional Bayesian inversion for geoacoustic profile estimation," Inverse Problems **30**(11), 114018.
Dosso, S. E., Morley, M. G., Giles, P. M., Brooke, G. H., McCammon, D. F., Pecknold, S., and Hines, P. C. (**2007**). "Spatial field shifts in ocean acoustic environmental sensitivity analysis," J. Acoust. Soc. Am. **122**(5), 2560–2570.
Dozier, L. B., and Tappert, F. D. (**1978a**). "Statistics of normal mode amplitudes in a random ocean. I. Theory," J. Acoust. Soc. Am. **63**(2), 353–365.
Dozier, L. B., and Tappert, F. D. (**1978b**). "Statistics of normal mode amplitudes in a random ocean. II. Computations," J. Acoust. Soc. Am. **64**(2), 533–547.
Duda, T. F., Lin, Y.-T., Newhall, A. E., Helfrich, K. R., Lynch, J. F., Zhang, W. G., Lermusiaux, P. F. J., and Wilkin, J. (**2019**). "Multiscale multiphysics data-informed modeling for three-dimensional ocean acoustic simulation and prediction," J. Acoust. Soc. Am. **146**(3), 1996–2015.
Dutt, A., Subramani, D. N., Kulkarni, C. S., and Lermusiaux, P. F. J. (**2018**). "Clustering of massive ensemble of vehicle trajectories in strong, dynamic and uncertain ocean flows," in *Proceedings of the OCEANS Conference 2018*, May 28–31, Charleston, SC.
Elisseeff, P., Schmidt, H., and Xu, W. (**2002**). "Ocean acoustic tomography as a data assimilation problem," IEEE J. Oceanic Eng. **27**(2), 275–282.
El Moçayd, N., Mohamed, M. S., Ouazar, D., and Seaid, M. (**2020**). "Stochastic model reduction for polynomial chaos expansion of acoustic waves using proper orthogonal decomposition," Rel. Eng. Syst. Safety **195**, 106733.
Etter, P. C. (**2018**). *Underwater Acoustic Modeling and Simulation* (CRC Press, Boca Raton, FL).
Evangelinos, C., Lermusiaux, P. F. J., Xu, J., Haley, P. J., and Hill, C. N. (**2009**). "Many task computing for multidisciplinary ocean sciences: Real-time uncertainty prediction and data assimilation," in *Proceedings of the 2nd Workshop on Many-Task Computing on Grids and Supercomputers*, November 16, Portland, OR.
Evangelinos, C., Lermusiaux, P. F. J., Xu, J., Haley, P. J., and Hill, C. N. (**2011**). "Many task computing for real-time uncertainty prediction and data assimilation in the ocean," IEEE Trans. Parallel Distrib. Syst. **22**(6), 1012–1024.
Evans, R. B. (**1983**). "A coupled mode solution for acoustic propagation in a waveguide with stepwise depth variations of a penetrable bottom," J. Acoust. Soc. Am. **74**(1), 188–195.
Fabre, J. P., and Wood, W. T. (**2013**). "Uncertainty of transmission loss due to small scale fluctuations of sound speed in two environments," Proc. Mtgs. Acoust. **19**(1), 005008.
Feppon, F., and Lermusiaux, P. F. J. (**2018a**). "Dynamically orthogonal numerical schemes for efficient stochastic advection and Lagrangian transport," SIAM Rev. **60**(3), 595–625.
Feppon, F., and Lermusiaux, P. F. J. (**2018b**). "A geometric approach to dynamical model-order reduction," SIAM J. Matrix Anal. Appl. **39**(1), 510–538.
Feppon, F., and Lermusiaux, P. F. J. (**2019**). "The extrinsic geometry of dynamical systems tracking nonlinear matrix projections," SIAM J. Matrix Anal. Appl. **40**(2), 814–844.
Feynman, R., and Hibbs, A. (**1965**). *Quantum Mechanics and Path Integrals* (Dover, New York).

Finette, S. (**2005**). "Embedding uncertainty into ocean acoustic propagation models (L)," J. Acoust. Soc. Am. **117**(3), 997–1000.
Finette, S. (**2006**). "A stochastic representation of environmental uncertainty and its coupling to acoustic wave propagation in ocean waveguides," J. Acoust. Soc. Am. **120**(5), 2567–2579.
Firing, E., and Gordon, R. L. (**1990**). "Deep ocean acoustic Doppler current profiling," in *Proceedings of the IEEE Fourth Working Conference on Current Measurement*, April 3–5, Clinton, MD, pp. 192–201.
Flatté, S. M. (**1983**). "Wave propagation through random media: Contributions from ocean acoustics," Proc. IEEE **71**(11), 1267–1294.
Gartner, J. W. (**2004**). "Estimating suspended solids concentrations from backscatter intensity measured by acoustic Doppler current profiler in San Francisco Bay, California," Mar. Geology **211**(3–4), 169–187.
Gemba, K. L., Vazquez, H. J., Sarkar, J., Tippman, J. D., Cornuelle, B., Hodgkiss, W. S., and Kuperman, W. (**2022**). "Moving source ocean acoustic tomography with uncertainty quantification using controlled source-tow observations," J. Acoust. Soc. Am. **151**(2), 861–880.
Gerdes, F., and Finette, S. (**2012**). "A stochastic response surface formulation for the description of acoustic propagation through an uncertain internal wave field," J. Acoust. Soc. Am. **132**(4), 2251–2264.
Gerstoft, P., and Mecklenbräuker, C. F. (**1998**). "Ocean acoustic inversion with estimation of a posteriori probability distributions," J. Acoust. Soc. Am. **104**(2), 808–819.
Ghanem, R. G., and Spanos, P. D. (**2003**). *Stochastic Finite Elements: A Spectral Approach* (Courier Corporation, New York).
Gupta, A., Ali, W. H., and Lermusiaux, P. F. J. (**2016**). "Boundary conditions for stochastic DO equations," MSEAS Report (MIT, Cambridge, MA).
Gupta, A., and Lermusiaux, P. F. J. (**2023**). "Bayesian learning of coupled biogeochemical-physical models," Prog. Oceanogr. **216**, 103050.
Harrison, C. H., and Harrison, J. A. (**1995**). "A simple relationship between frequency and range averages for broadband sonar," J. Acoust. Soc. Am. **97**(2), 1314–1317.
Heaney, K. D., and Campbell, R. L. (**2016**). "Three-dimensional parabolic equation modeling of mesoscale eddy deflection," J. Acoust. Soc. Am. **139**(2), 918–926.
Heuss, J. P., Haley, P. J., Jr., Mirabito, C., Coelho, E., Schönau, M. C., Heaney, K., and Lermusiaux, P. F. J. (**2020**). "Reduced order modeling for stochastic prediction onboard autonomous platforms at sea," in *Proceedings of Oceans 2020 IEEE/MTS*, October 5–14, Singapore, pp. 1–10.
Humara, M. J., Ali, W. H., Charous, A., Bhabra, M., and Lermusiaux, P. F. J. (**2022**). "Stochastic acoustic ray tracing with dynamically orthogonal differential equations," in *Proceeding of Oceans 2022 IEEE/MTS*, October 17–20, Hampton Roads, VA, pp. 1–10.
Ishimaru, A. (**1978**). *Wave Propagation and Scattering in Random Media* (Academic Press, New York).
Jagannathan, S., Bertsatos, I., Symonds, D., Chen, T., Nia, H. T., Jain, A. D., Andrews, M., Gong, Z., Nero, R., Ngor, L., Jech, M., Godo, O. R., Lee, S., Ratilal, P., and Makris, N. (**2009**). "Ocean Acoustic Waveguide Remote Sensing (OAWRS) of marine ecosystems," Mar. Ecol. Prog. Ser. **395**, 137–160.
Jakobsson, M., Allen, G., Carbotte, S., Falconer, R., Ferrini, V., Marks, K., Mayer, L., Rovere, M., Schmitt, T., Weatherall, P., and Wigley, R. (**2017**). "The Nippon Foundation GEBCO seabed 2030: Roadmap for future ocean floor mapping," Nippon Foundation, Tokyo, Japan.
James, K. R., and Dowling, D. R. (**2005**). "A probability density function method for acoustic field uncertainty analysis," J. Acoust. Soc. Am. **118**(5), 2802–2810.
James, K. R., and Dowling, D. R. (**2008**). "A method for approximating acoustic-field-amplitude uncertainty caused by environmental uncertainties," J. Acoust. Soc. Am. **124**(3), 1465–1476.
James, K. R., and Dowling, D. R. (**2011**). "Pekeris waveguide comparisons of methods for predicting acoustic field amplitude uncertainty caused by a spatially uniform environmental uncertainty (L)," J. Acoust. Soc. Am. **129**(2), 589–592.
Jensen, F. B., Kuperman, W. A., Porter, M. B., and Schmidt, H. (**2011**). *Computational Ocean Acoustics* (Springer Science & Business Media, New York).
Jourdain, G., Eriksson, L.-E., Kim, S. H., and Sohn, C. H. (**2013**). "Application of dynamic mode decomposition to acoustic-modes identification and damping in a 3-dimensional chamber with baffled injectors," J. Sound Vib. **332**(18), 4308–4323.
Khazaie, S., Wang, X., Komatitsch, D., and Sagaut, P. (**2019**). "Uncertainty quantification for acoustic wave propagation in a shallow water environment," Wave Motion **91**, 102390.
Khine, Y. Y., Creamer, D. B., and Finette, S. (**2010**). "Acoustic propagation in an uncertain waveguide environment using stochastic basis expansions," J. Comput. Acoust. **18**(4), 397–441.
Koch, O., and Lubich, C. (**2007**). "Dynamical low-rank approximation," SIAM J. Matrix Anal. Appl. **29**(2), 434–454.
Lavery, A. C., Wiebe, P. H., Stanton, T. K., Lawson, G. L., Benfield, M. C., and Copley, N. (**2007**). "Determining dominant scatterers of sound in mixed zooplankton populations," J. Acoust. Soc. Am. **122**(6), 3304–3326.
Le Maître, O., and Knio, O. M. (**2010**). *Spectral Methods for Uncertainty Quantification: With Applications to Computational Fluid Dynamics* (Springer Science & Business Media, New York).
Le Maître, O. P., Knio, O. M., Najm, H. N., and Ghanem, R. G., (**2001**). "A stochastic projection method for fluid flow: I. Basic formulation," J. Comput. Phys. **173**(2), 481–511.
Lee, B. M., Johnson, J. R., and Dowling, D. R. (**2022**). "Predicting acoustic transmission loss uncertainty in ocean environments with neural networks," J. Mech. Sci. Eng. **10**(10), 1548.
Lermusiaux, P. F. J. (**1999**). "Data assimilation via error subspace statistical estimation, Part II: Mid-Atlantic Bight shelfbreak front simulations, and ESSE validation," Mon. Wea. Rev. **127**(7), 1408–1432.
Lermusiaux, P. F. J. (**2006**). "Uncertainty estimation and prediction for interdisciplinary ocean dynamics," J. Comput. Phys. **217**(1), 176–199.
Lermusiaux, P. F. J. (**2007**). "Adaptive modeling, adaptive data assimilation and adaptive sampling," Phys. D: Nonlinear Phenom. **230**(1), 172–196.
Lermusiaux, P. F. J., and Chiu, C.-S. (**2002**). "Four-dimensional data assimilation for coupled physical-acoustical fields," in *Acoustic Variability 2002*, edited by N. G. Pace and F. B. Jensen (Kluwer Academic Press, Philadelphia, PA), pp. 417–424.
Lermusiaux, P. F. J., Chiu, C.-S., Gawarkiewicz, G. G., Abbot, P., Robinson, A. R., Miller, R. N., Haley, P. J., Jr., Leslie, W. G., Majumdar, S. J., Pang, A., and Lekien, F. (**2006**). "Quantifying uncertainties in ocean predictions," Oceanography **19**(1), 90–105.
Lermusiaux, P. F., Chiu, C.-S., and Robinson, A. R. (**2002**). "Modeling uncertainties in the prediction of the acoustic wavefield in a shelfbreak environment," in *Proceedings of the 5th International Conference on Theoretical and Computational Acoustics*, edited by E.-C. Shang, Q. Li, and T. F. Gao (World Scientific Publishing Co., Singapore), pp. 191–200.
Lermusiaux, P. F. J., Haley, P. J., Jr., Mirabito, C., Ali, W. H., Bhabra, M., Abbot, P., Chiu, C.-S., and Emerson, C. (**2020a**). "Multi-resolution probabilistic ocean physics-acoustic modeling: Validation in the New Jersey continental shelf," in *Oceans 2020 IEEE/MTS*, October 5–14, Singapore, pp. 1–9.
Lermusiaux, P. F. J., Mirabito, C., Haley, P. J., Jr., Ali, W. H., Gupta, A., Jana, S., Dorfman, E., Laferriere, A., Kofford, A., Shepard, G., Goldsmith, M., Heaney, K., Coelho, E., Boyle, J., Murray, J., Freitag, L., and Morozov, A. (**2020b**). "Real-time probabilistic coupled ocean physics-acoustics forecasting and data assimilation for underwater GPS," in *Oceans 2020 IEEE/MTS*, October 5–14, Singapore.
Lermusiaux, P. F. J., and Robinson, A. R. (**1999**). "Data assimilation via error subspace statistical estimation, Part I: Theory and schemes," Mon. Weather Rev. **127**(7), 1385–1407.
Lermusiaux, P. F. J., Xu, J., Chen, C.-F., Jan, S., Chiu, L., and Yang, Y.-J. (**2010**). "Coupled ocean–acoustic prediction of transmission loss in a continental shelfbreak region: Predictive skill, uncertainty quantification, and dynamical sensitivities," IEEE J. Oceanic Eng. **35**(4), 895–916.
Lin, J., and Lermusiaux, P. F. J. (**2021**). "Minimum-correction second-moment matching: Theory, algorithms and applications," Numer. Math. **147**(3), 611–650.
Lin, Y.-T., Duda, T. F., and Newhall, A. E. (**2013**). "Three-dimensional sound propagation models using the parabolic-equation approximation and the split-step fourier method," J. Comput. Acoust. **21**(01), 1250018.
Liu, J. S. (**2008**). *Monte Carlo Strategies in Scientific Computing* (Springer Science & Business Media, New York).
Loeve, M. (**1978**). *Probability Theory II* (Springer, New York).
Lolla, T., and Lermusiaux, P. F. J. (**2017a**). "A Gaussian mixture model smoother for continuous nonlinear stochastic dynamical systems: Applications," Mon. Weather Rev. **145**, 2763–2790.
Lolla, T., and Lermusiaux, P. F. J. (**2017b**). "A Gaussian mixture model smoother for continuous nonlinear stochastic dynamical systems: Theory and scheme," Mon. Weather Rev. **145**, 2743–2761.

Lu, P., and Lermusiaux, P. F. J. (**2021**). "Bayesian learning of stochastic dynamical models," Phys. D **427**, 133003.
MacLennan, D. N., and Simmonds, E. J. (**2013**). *Fisheries Acoustics* (Springer Science & Business Media, New York).
Makris, N. C., Ratilal, P., Symonds, D. T., Jagannathan, S., Lee, S., and Nero, R. W. (**2006**). "Fish population and behavior revealed by instantaneous continental shelf-scale imaging," Science **311**(5761), 660–663.
McDaniel, S. T. (**1982**). "Mode coupling due to interaction with the seabed," J. Acoust. Soc. Am. **72**(3), 916–923.
Medwin, H., and Clay, C. S. (**1998**). "Chapter 1 - The realm of acoustical oceanography; theory and applications of ocean acoustics," in *Fundamentals of Acoustical Oceanography*, Applications of Modern Acoustics, edited by H. Medwin and C. S. Clay (Academic Press, San Diego), pp. 1 – VI.
Michalopoulou, Z.-H., Gerstoft, P., Kostek, B., and Roch, M. A. (**2021**). "Introduction to the special issue on machine learning in acoustics," J. Acoust. Soc. Am. **150**(4), 3204–3210.
Miller, R. N. (**2007**). "Topics in data assimilation: Stochastic processes," Phys. D **230**(1–2), 17–26.
Morozov, A. K., and Colosi, J. A. (**2017**). "Equations for normal-mode statistics of sound scattering by a rough elastic boundary in an underwater waveguide, including backscattering," J. Acoust. Soc. Am. **142**(3), EL292–EL298.
Munk, W., and Wunsch, C. (**1979**). "Ocean acoustic tomography: A scheme for large scale monitoring," Deep Sea Res. Part A **26**(2), 123–161.
Najm, H. N. (**2009**). "Uncertainty quantification and polynomial chaos techniques in computational fluid dynamics," Annu. Rev. Fluid Mech. **41**, 35–52.
Patterson, B., and Dowling, D. R. (**2017**). "Estimation of the probability density function of transmission loss in the ocean using area statistics," J. Acoust. Soc. Am. **142**(4), 2525–2525.
Pekeris, C. L. (**1948**). "Theory of propagation of explosive sound in shallow water," in *Propagation of Sound in the Ocean* (Geological Society of America, Boulder, CO).
Pierce, A. D. (**1965**). "Extension of the method of normal modes to sound propagation in an almost–stratified medium," J. Acoust. Soc. Am. **37**(1), 19–27.
Pope, S. B. (**2000**). *Turbulent Flows* (Cambridge University Press, Cambridge, UK).
Porter, M. (**1991**). "The Kraken normal mode program," Report No. SM-245 (Saclant Undersea Research Center, La Spezia, Italy).
Porter, M. B. (**2010**). "Open–source software for modeling sound propagation in the ocean," J. Acoust. Soc. Am. **128**, 2299.
Quazi, A. (**1981**). "An overview on the time delay estimate in active and passive systems for target localization," IEEE Trans. Acoust. Speech, Signal Process. **29**(3), 527–533.
Ratilal, P., and Makris, N. C. (**2005**). "Mean and covariance of the forward field propagated through a stratified ocean waveguide with three-dimensional random inhomogeneities," J. Acoust. Soc. Am. **118**(6), 3532–3559.
Rixen, M., Lermusiaux, P. F. J., and Osler, J. (**2012**). "Quantifying, predicting, and exploiting uncertainties in marine environments," Ocean Dyn. **62**(3), 495–499.
Robinson, A. R., Abbot, P., Lermusiaux, P. F. J., and Dillman, L. (**2002**). "Transfer of uncertainties through physical-acoustical-sonar end-to-end systems: A conceptual basis," in *Acoustic Variability, 2002*, edited by N. G. Pace and F. B. Jensen (Kluwer Academic Press, Philadelphia, PA), pp. 603–610.
Robinson, A. R., and Lermusiaux, P. F. J (**2004**). "Prediction systems with data assimilation for coupled ocean science and ocean acoustics," in *Proceedings of the Sixth International Conference on Theoretical and Computational Acoustics*, August 11–15, Honolulu, HI, pp. 325–342.
Rouseff, D., Turgut, A., Wolf, S. N., Finette, S., Orr, M. H., Pasewark, B. H., Apel, J. R., Badiey, M., Chiu, C-s., Headrick, R. H., Lynch, J. F., Kemp, J. N., Newhall, A. E., von der Heydt, K., and Tielbuerger, D. (**2002**). "Coherence of acoustic modes propagating through shallow water internal waves," J. Acoust. Soc. Am. **111**(4), 1655–1666.
Rytov, S. M., Kravtsov, Y. A., and Tatarskii, V. I. (**1987**). *Principles of Statistical Radiophysics 1. Elements of Random Process Theory* (Springer, New York).
Ryu, T., Ali, W. H., Haley, P. J., Jr., Mirabito, C., Charous, A., and Lermusiaux, P. F. J. (**2022**). "Incremental low-rank dynamic mode decomposition model for efficient dynamic forecast dissemination and onboard forecasting," in *Proceeding of Oceans 2022 IEEE/MTS*, October 17–20, Hampton Roads, VA, pp. 1–8.
Ryu, T., Heuss, J. P., Haley, P. J., Jr., Mirabito, C., Coelho, E., Hursky, P., Schönau, M. C., Heaney, K., and Lermusiaux, P. F. J. (**2021**). "Adaptive stochastic reduced order modeling for autonomous ocean platforms," in *Proceedings of Oceans 2021 IEEE/MTS*, September 20–23, San Diego, CA, pp. 1–9.
Sapsis, T. P., and Lermusiaux, P. F. J. (**2009**). "Dynamically orthogonal field equations for continuous stochastic dynamical systems," Phys. D **238**(23–24), 2347–2360.
Sapsis, T. P., and Lermusiaux, P. F. J. (**2012**). "Dynamical criteria for the evolution of the stochastic dimensionality in flows with uncertainty," Phys. D **241**(1), 60–76.
Schmid, P. J. (**2022**). "Dynamic mode decomposition and its variants," Annu. Rev. Fluid Mech. **54**, 225–254.
Shorey, J., Nolte, L., and Krolik, J. (**1994**). "Computationally efficient Monte Carlo estimation algorithms for matched field processing in uncertain ocean environments," J. Comput. Acoust. **02**(03), 285–314.
Smith, K. B., and Tappert, F. D. (**1993**). "UMPE: The University of Miami Parabolic Equation model. Version 1.0," University of Miami, Miami, FL.
Sondergaard, T., and Lermusiaux, P. F. J. (**2013a**). "Data assimilation with Gaussian mixture models using the dynamically orthogonal field equations. Part I: Theory and scheme," Mon. Weather Rev. **141**(6), 1737–1760.
Sondergaard, T., and Lermusiaux, P. F. J. (**2013b**). "Data assimilation with Gaussian mixture models using the dynamically orthogonal field equations. Part II: Applications," Mon. Weather Rev. **141**(6), 1761–1785.
Stojanovic, M. (**1996**). "Recent advances in high-speed underwater acoustic communications," IEEE J. Oceanic Eng. **21**(2), 125–136.
Sturm, F., and Fawcett, J. A. (**2003**). "On the use of higher-order azimuthal schemes in 3-D PE modeling," J. Acoust. Soc. Am. **113**(6), 3134–3145.
Subramani, D., and Lermusiaux, P. F. J. (**2024**). "Probabilistic ocean predictions with dynamically-orthogonal primitive equations," in preparation.
Tappert, F. D. (**1977**). "The parabolic approximation method," in *Wave Propagation and Underwater Acoustics*, edited by J. B. Keller and J. S. Papadakis (Springer, New York), p. 224.
Tatarskii, V. I. (**1971**). "The effects of the turbulent atmosphere on wave propagation" (Israel Program for Scientific Translations, Jerusalem, Israel).
Thorsos, E. I., Henyey, F. S., Elam, W. T., Hefner, B. T., Reynolds, S. A., and Yang, J. (**2010**). "Transport theory for shallow water propagation with rough boundaries," AIP Conf. Proc. **1272**(1), 99–105.
Tollefsen, C. D. S. (**2021**). "Predicting acoustic variability: Pragmatic considerations for selecting a stochastic or deterministic approach," IEEE J. Oceanic Eng. **46**(3), 1045–1056.
Tolstoy, A. (**1993**). *Matched Field Processing for Underwater Acoustics* (World Scientific, Singapore).
Tolstoy, A. (**1996**). "3-D propagation issues and models," J. Comput. Acoust. **04**(03), 243–271.
Ueckermann, M. P., and Lermusiaux, P. F. J. (**2012**). "2.29 finite volume MATLAB framework documentation," MSEAS Report No. 14 (MIT, Cambridge, MA).
Ueckermann, M. P., Lermusiaux, P. F. J., and Sapsis, T. P. (**2013**). "Numerical schemes for dynamically orthogonal equations of stochastic fluid and ocean flows," J. Comput. Phys. **233**, 272–294.
Uscinski, B. J. (**1977**). *The Elements of Wave Propagation in Random Media* (McGraw-Hill Companies, New York).
Wang, D., Lermusiaux, P. F. J., Haley, P. J., Jr., Eickstedt, D., Leslie, W. G., and Schmidt, H. (**2009**). "Acoustically focused adaptive sampling and on-board routing for marine rapid environmental assessment," J. Mar. Syst. **78**, S393–S407.
Xiu, D., and Karniadakis, G. E. (**2003**). "Modeling uncertainty in flow simulations via generalized polynomial chaos," J. Comput. Phys. **187**(1), 137–167.
Xiu, D., Lucor, D., Su, C.-H., and Karniadakis, G. E. (**2002**). "Stochastic modeling of flow-structure interactions using generalized polynomial chaos," J. Fluids Eng. **124**(1), 51–59.
Yilmaz, N. K., Evangelinos, C., Patrikalakis, N. M., Lermusiaux, P. F. J., Haley, P. J., Leslie, W. G., Robinson, A. R., Wang, D., and Schmidt, H. (**2006**). "Path planning methods for adaptive sampling of environmental and acoustical ocean fields," in *Proceedings of Oceans 2006*, September 18–21, Boston, MA.
Zingarelli, R. A. (**2008**). "A mode-based technique for estimating uncertainty in range-averaged transmission loss results from underwater acoustic calculations," J. Acoust. Soc. Am. **124**(4), EL218– EL222.